

JLAB

Commissioning and calibration the CLAS12 Silicon Vertex Tracker (SVT)

v1.2

Yuri Gotra

6/12/2013

Table of Contents

1	Introduction	5
2	SVT module quality assurance tests	6
2.1	Test set-ups	9
2.2	Sensor current	9
2.3	Digital tests	9
2.3.1	Module communication	10
2.3.2	Channel masking.....	10
2.3.3	Front-end calibration.....	10
2.4	Analog tests.....	11
2.4.1	Reconstruction of the analog strip response	12
2.4.2	Noise and gain measurement	14
2.5	Burn-in test.....	21
2.6	Module problem summary	21
2.6.1	Defective channels results.....	21
3	SVT configuration, conditions, and alignment databases.....	21
4	SVT commissioning during tracker assembling	22
4.1	Module construction	22
4.2	Barrel assembly.....	24
4.3	Readout hardware configurations	25
4.3.1	Two module configuration.....	26
4.3.2	Configuration of test sector.....	26
4.3.3	Configuration for barrel	27
4.4	Noise measurements	27
4.4.1	Measurement of common mode noise	27
4.4.2	Closely separated triggers	35
4.4.3	Synchronous trigger test	35
4.5	Calibration procedure.....	36
4.5.1	Scan production	36
4.5.2	Fitting service.....	37
4.5.3	Analysis service	37
4.5.4	Archiving service	37
4.5.5	Module indexing schemes.....	37

4.6	SVT commissioning and cosmic ray tests	38
4.7	Beam tests with SVT modules	40
4.7.1	Beam test goals	40
4.7.2	Test setups.....	41
4.7.3	Beam telescope	42
4.7.4	Cooling.....	43
4.7.5	Alignment	43
4.7.6	Track reconstruction	44
4.7.7	Event selection.....	44
4.7.8	Efficiency and noise occupancy.....	45
4.7.9	Spatial resolution	46
4.7.10	Median charge.....	46
4.7.11	Detector Bias Voltage	47
4.7.12	Charge collection in the inter-strip region	48
4.7.13	Incidence angle and magnetic field.....	48
4.7.14	Edge measurements	49
4.7.15	Timing measurements	49
5	Detector control and safety system (DCS).....	50
5.1	Monitoring of SVT Operating Parameters.....	50
5.2	Calibration of Detectors and Readout Electronics.....	51
6	Data Quality Monitoring.....	52
6.1	DQM architecture	52
6.2	DQM Operation	53
6.3	History plotting tool for DQM	54
6.4	Interactive SVG Maps and Web Services for SVT monitoring.....	55
7	Module services	57
7.1	Power supplies	57
7.2	Cables.....	57
7.3	Cooling.....	58
8	Tracker integration and commissioning in Hall B	58
8.1	Transportation requirements	58
8.2	Tracker integration tests.....	58
8.3	Mechanical stability and alignment	59

8.4	Commissioning the SVT control and readout systems	61
8.4.1	The control and readout systems.....	61
8.4.2	Checkout of the detector components and cabling	62
8.4.3	SVT slow controls.....	62
8.4.4	Relative synchronization of the front-end.....	62
8.4.5	Calibration of the readout system gain	62
8.4.6	Cosmic ray calibration	63
8.5	Performance of the local reconstruction	63
8.5.1	Occupancy.....	63
8.5.2	Signal-to-noise ratio.....	63
8.5.3	Gain calibration.....	64
8.5.4	Lorentz angle measurement	64
8.5.5	Hit efficiency	64
9	Online software.....	64
10	SVT DAQ system and commissioning software	65
11	Data samples and Monte Carlo simulations.....	66
12	Track reconstruction	66
12.1	Track reconstruction algorithms	67
12.2	Track reconstruction efficiency	67
12.2.1	Track reconstruction efficiency using muons triggered by the CTOF	67
12.2.2	Track reconstruction efficiency using tracker data only	68
12.3	Track parameter resolution	68
12.4	Hit resolution	68
12.5	Vertex reconstruction.....	69
13	Checkout with beam	69
Bibliography	70	
Detector Commissioning Information	71	

1 Introduction

This document describes the procedures that will be followed to commission the CLAS12 Silicon Vertex Tracker (SVT) and all its components. The goal of these procedures is to ensure the quality standards defined by the Technical Design Report (TDR) of the detector; optimize the sequence of operations during construction, installation, and operation in terms of time, manpower, and computing resources; ensure the proper functioning of the SVT before and after installation in Hall B; obtain initial calibration data necessary for the reconstruction of the physics events; determine the performance of the SVT; and optimize the overall detector configuration according to the requirement of the physics runs.

The aim of the tracker is to measure the trajectories of charged particles (tracks) with excellent momentum, angle, and positional resolution, and with high pattern reconstruction efficiency.

Following the CLAS12 commissioning plan, SVT commissioning will be divided in three phases: quality assurance and system checkout, commissioning without beam, and commissioning with beam. CLAS12 central detector is shown in Figure 1.

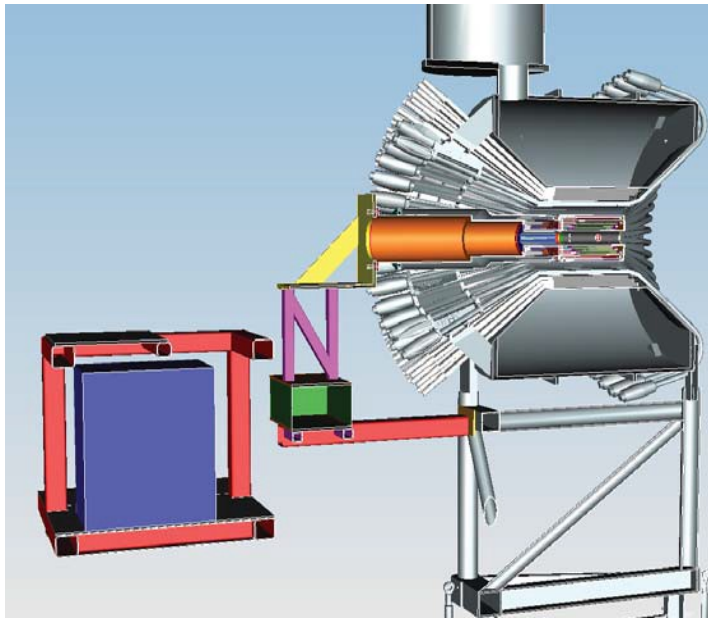


Figure 1. Clas12 central detector

The first phase, quality assurance and system checkout of the detector, will consist of the procedures that will be applied, before and during the assembly, to check that all detector components are consistent with specifications and to ensure the proper functioning of the whole tracker before and after installation in Hall B. In particular, the quality assurance procedures will include tests on specific system components, such as modules, cables, and electronics boards, to measure their characteristics, to check compliance with the specified requirements, to verify that active components are responding correctly, and to identify and replace faulty elements. System checkout procedures will be performed upon completion of the system assembly. These procedures will include alignment and

verification of the system positioning, as well as tests of high and low voltage systems, front-end electronics, readout electronics, data acquisition, and the trigger system.

The second phase of the SVT commissioning will focus on the verification of the SVT performance, after completion of the checkout procedures and before the beginning of the on-beam operation. The purpose of the associated procedures will be to optimize the system configuration, determine the initial calibration that will be later used in the reconstruction algorithm, and verify that the system performance is consistent with the design goals, which will be achieved by data-taking in special configurations, exploiting dedicated equipment, as well as using cosmic rays. Data will be collected in different configurations of the CLAS12 magnet, data acquisition, and trigger to obtain the maximum information as requested by the SVT group.

The final phase of the commissioning will be performed upon beam delivery in Hall B. The commissioning of the SVT will be performed using the optimal configurations of beam energy and intensity, CLAS12 magnet, CLAS12 data acquisition and trigger. The accumulated data will be used to verify the response of the tracker to specific reactions, measure noise figures and rates, and determine the final detector calibration used by the CLAS12 reconstruction software.

2 SVT module quality assurance tests

This section describes the module performance tests that are done at various stages during module production at FNAL, assembly of the SVT at JLab, and debugging problems on a module level during tracker integration and commissioning. This includes tests of the sensor current behavior, the digital and analog functionalities of the module readout chips, and the equivalent noise charge on the silicon strips. The test results must show that the modules perform well within their requirements. All test results are documented and remain an important reference for the module performance during the lifetime of the detector.

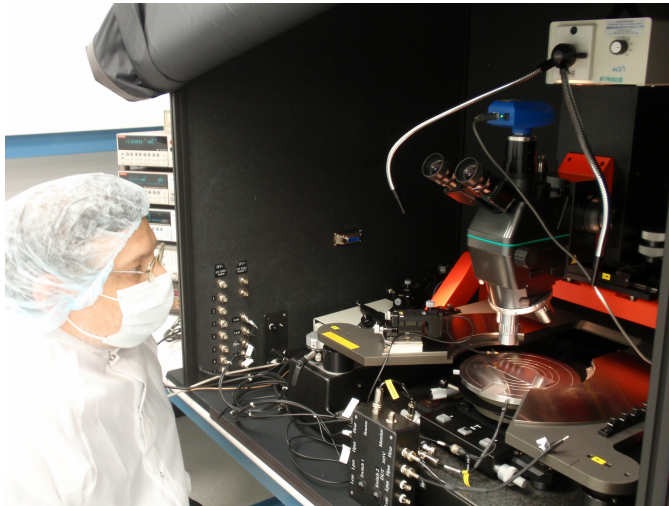


Figure 2. Probe station for sensor qualification measurements.

For testing of the SVT module, a series of tests are planned. The goal of the performance tests is to check the functionality of each of the modules. These tests include measurements of:

- **Sensor current:** Check that the sensor behaves like a diode and can be fully depleted. The maximum allowed leakage current is 10 nA/cm^2 (470 nA per sensor). Test stand for sensor measurements is shown in Figure 2.
- **Analog functionality of the module electronics:** Test the readout of the strips and ensure that at least 99% of all silicon strips can be read out and the noise on the strips agrees with the expected value for that module.
- **Digital functionality of the module electronics:** Check that the data can be read out by the data acquisition system. In addition, the channel masking and chip basic functionality is tested.

The main test stages during the SVT assembly and integration:

- **Module production at FNAL:** The position resolution of the detector can be compromised if the alignment is not well known. Strict positional tolerances are imposed so that minimal corrections need to be made to physics measurements. Therefore, both the position of the sensors with respect to each other and with respect to alignment points are measured and controlled during module production. A mechanical survey and metrology are carried out before electrical testing. The metrology of the module checks whether the module fits within a well-defined envelope. This ensures that a module will have no interference with other modules, both while on the support structure and particularly during mounting, where module separation reaches a minimum.

Quality Assurance (QA) testing of module components is described in CLAS-Note 2010-016, *CLAS12 Silicon Vertex Tracker Quality Assurance / Quality Control*.

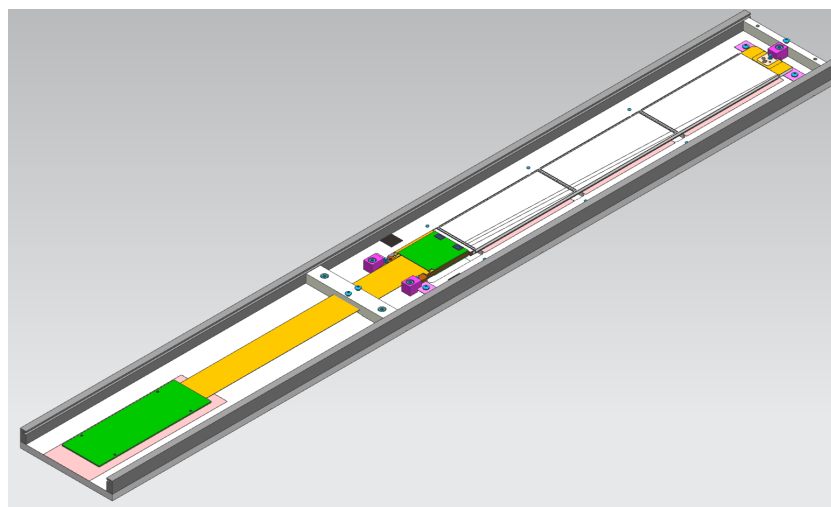


Figure 3. SVT module storage box.

Prerequisite for the module assembly is the QA test of the HFCB, after chip wire bonding (before encapsulation). This test is done at the dedicated test station at the Silicon Detector Facility (SiDet), FNAL. Full electrical functionality of all the

channels is verified, and Equivalent Noise Charge (ENC) data are recorded for every chip in a database, along with total current consumption on the low voltage lines. Additionally, a basic functionality test is done after encapsulation of chip-to-HFCB wire bonds. Immediately after module assembly, the module is tested in the clean room at SiDet. The aim is to identify defects in the modules as early as possible in production, so that effort is not expended on faulty modules and to provide an opportunity to fix the defect. Problematic modules are returned to the production line for repair while the modules passed QA tests are shipped to JLAB in the same storage/carrier box that was used for testing (Figure 3). In this box, the module could be powered, cooled, and operated under similar conditions as in the CLAS12 experiment. The box is constructed to provide access to both sides of the module to facilitate inspection and debugging. The box is closed off during the testing to prevent ambient light from falling on the silicon sensors.

- **JLab reception test:** After arrival at JLab, all modules are tested to check whether any new problems developed during handling and transport.
- **Assembly:** After placement of each module on the support, all the modules on the support are re-tested, to find and resolve problems with cables routed on the outside of the cylinder. Problematic modules are replaced with spares.
- **Final commissioning:** After installation in Hall B, the SVT is tested to check that no problems have occurred during installation of the detector and to test the connections with the readout systems in the services caverns. A series of physics runs are performed with and without the beam and magnetic field.

At each of these four stages, the tests for the module performance (described later in this chapter) are repeated. Tests at later stages are aimed at finding problems with data acquisition and services, such as the power supplies and cables, and ensuring that no common mode noise was added to the system due to grounding/shielding problems.

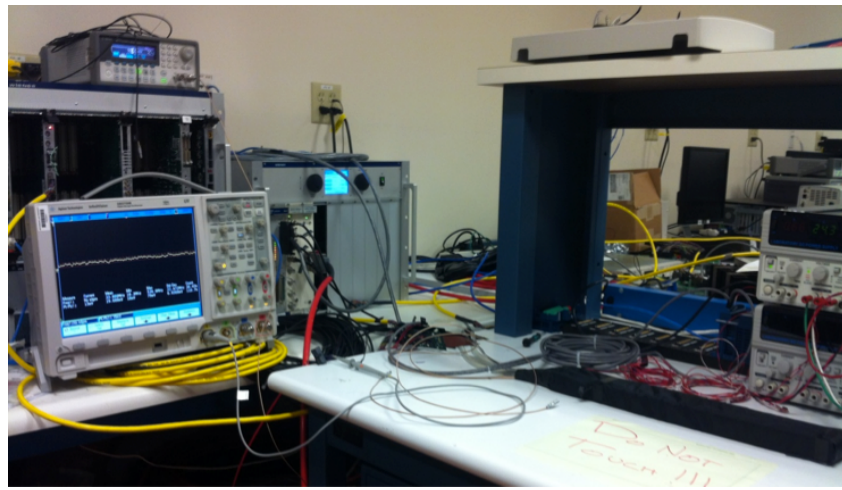


Figure 4. SVT module test stand. Two modules wrapped in light-tight fabric on the right side are connected to the VME readout board.

2.1 Test set-ups

Modules are transported to JLab mounted inside the carrier boxes. Upon arrival, the modules are re-tested on a dedicated test stand located in the SVT clean room of the EEL building (

Figure 4).

After the reception tests, the modules are placed on the SVT support structure. After assembly at JLab is completed, a light-tight Faraday cage made from carbon fiber with segmented copper mesh will enclose the SVT with provision for dry air to be flushed through the SVT. The SVT protection cover is designed to safely transport the SVT from the EEL building to Hall B.

With the SVT in its final position in the CLAS12 detector, all the modules are re-tested with the actual services that are used to operate the SVT during data-taking.

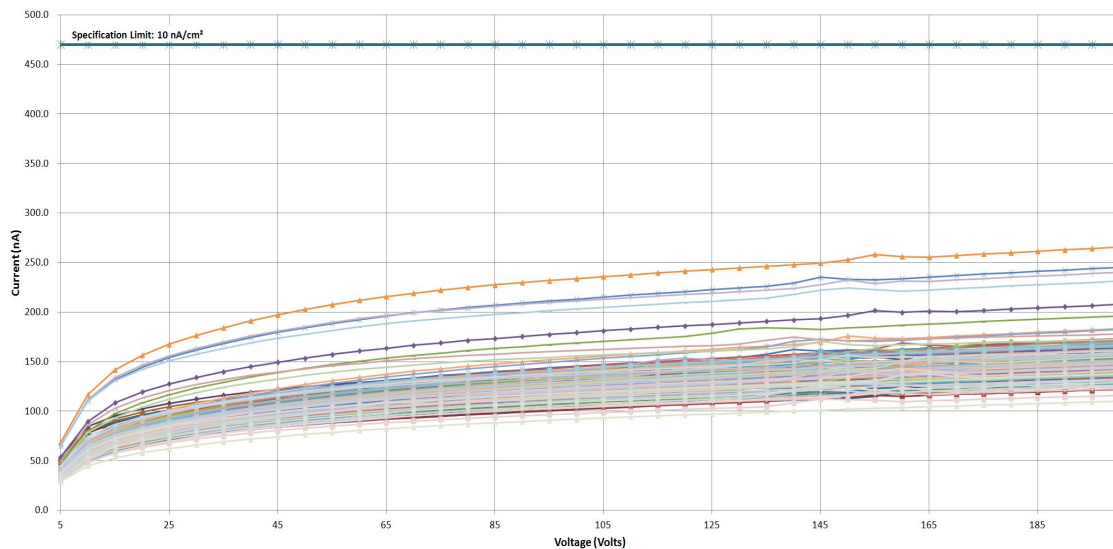


Figure 5. Measurements of the sensor leakage current for the intermediate SVT sensors. Horizontal line represents the maximum current defined by specifications on the sensors.

2.2 Sensor current

Reverse bias voltage is applied to a silicon sensor and the current is measured to check for breakdown problems (Figure 5). The reverse bias voltage induces a sensor current, which is composed of the generation current and the surface current. Generation current refers to the thermally induced charge in the depletion layer and is therefore proportional to the depletion volume, which is proportional to $\sqrt{V_{bias}}$. The surface current can be approximated by an Ohmic resistance. The sensor behavior is studied by plotting the measured leakage current *vs.* increasing values of the sensor bias voltage to form an IV-curve for each module. Each module uses three sensors, so the leakage current measured on the modules is the sum of the currents from multiple sensors.

2.3 Digital tests

The digital tests check functionality of the digital part of the FSSR2 chips on the module

and the ability to read out data from the module. All the tests are based on measuring the occupancy of each channel while varying a specific setting in the chip configuration. The correct cabling has to be verified before the digital tests take place, as problems with the module communication would lead to test failures.

2.3.1 Module communication

When first powered, basic communication is confirmed when the SVT modules write to the chip registers and read back the response. The front-end electronics is set up to return the contents of their configuration registers, so a known bit pattern can be expected. A hard-reset test checks the initialization of the modules. Once the module has been checked for basic power and readout functionality, the electrical performance can be tested.

2.3.2 Channel masking

The readout chips of the modules apply a mask to the measured hits on all the strips. A channel that is masked always returns “0”. Masking is necessary for strip channels with high noise, as unmasked noisy channels add fake hits and increase the amount of data that has to be read out.

To check the capability of the chips to turn a mask on and turn a mask off all the channels on the chips, the trigger occupancy is measured using different settings of the mask register. During the test, the output is set such that any channel which is not masked returns a signal corresponding to “1”. The test starts with a mask register where all channels are unmasked. For each consecutive mask register in the test, one more channel on each chip is masked, until all channels are masked at the final mask register. The result of this test is a 2D projection of a 3D histogram, where the shade of color indicates the trigger occupancy as a function of the channel number and the mask register.

If there is a channel that will need to be masked due to high noise, which also had a masking defect, it will have to be masked offline.

2.3.3 Front-end calibration

The binary threshold must be set so that a channel can reliably distinguish between the signal and noise. This means that the response to different signals must be known and the noise must be low enough to be cut out. The testing of SVT modules is a check of their calibration and performance and also of the test system itself. Figure 6 shows linearity test of the FSSR2 hit/no-hit discriminator DAC. The key to the characterization of the modules lies in reconstructing the analog response of the modules from the binary readout by first setting the optimal chip parameters for the charge injection, then injecting a set of charges into the front-end, and scanning through the threshold to map out the response curve. A full test sequence contains procedures that verify the digital performance of the chips. These exercise and test the channel mask registers and chip logic.

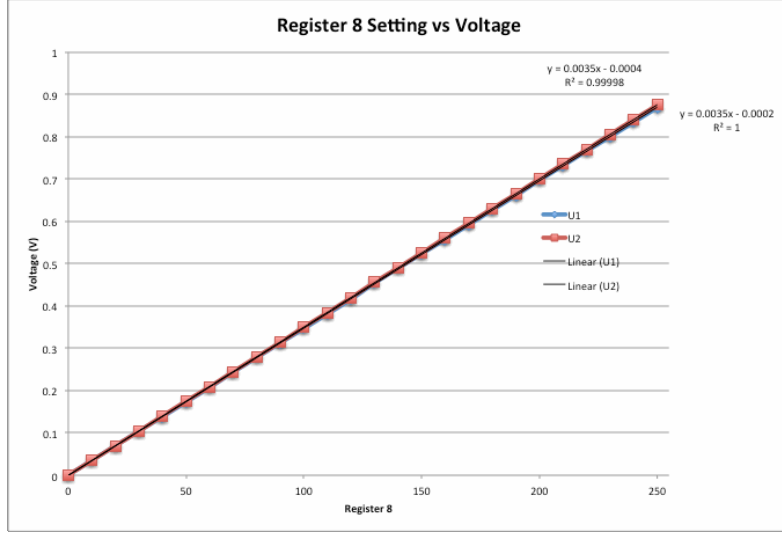


Figure 6. Calibration of FSSR2 hit/no hit discriminator DAC linearity.

2.4 Analog tests

In the analog stage, the signal induced in the strip is amplified, shaped, and discriminated using a threshold setting. There are physics-driven requirements for efficiency of 99% per strip (low false negatives) and noise occupancy of 10^{-3} (low false positives) at the nominal threshold. For data taking, the default setting of the threshold is chosen such that it corresponds to the output signal as created by an input signal equivalent to about 1 fC charge induced on the strip. A signal of 1 fC is well above the expected noise, and well below the average induced charge from the passage of a charge particle. To find the threshold corresponding to 1 fC, the analog response needs to be reconstructed for each channel. The loss of information from the binary readout system implies that the threshold set on a chip must have a well-known correspondence to the charge deposited in the detector. There is also a need for the threshold charge to be the same across the channels in a detector - if different channels responded differently to deposition of the nominal threshold charge, the track-finding algorithms would be biased by the potential extra hits. Any spread in the response among the different channels of a chip results in a spread of the efficiency and noise occupancy which degrades effective performance. This leads to a requirement that the channel-to-channel variations in threshold and noise are kept to a minimum.

The FSSR2 has a Base Line Restoration (BLR) circuit which can be turned on and off with BLR parameter. Typical pulse shape after the BLR is shown in Figure 7. To meet the specifications, the threshold dispersion of the FSSR2 chip has to be within 500 e for BLR ON setting (800 e for BLR OFF) as shown in Figure 8. A goal of the binary readout architecture is to keep the threshold spread negligible compared to the noise value for a full strip length. A comparison of the noise of 2000 electrons for 33 cm strips with the threshold spread of 500 electrons demonstrates that the threshold spread is negligible compared to noise and if such, it will not affect neither the efficiency nor the noise occupancy.

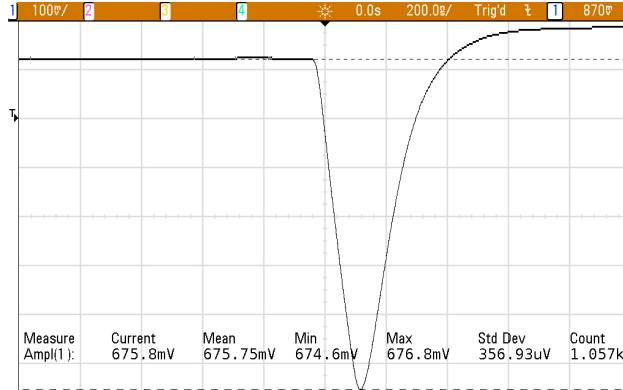


Figure 7. Single channel analog output pulse measured after the Base Line Restore circuit.

The active part of the SVT module is the silicon detector. It reacts to ionizing particles that pass through, generating a charge that is discriminated by the chips on the hybrid. The detector medium is a silicon crystal. The $320\text{ }\mu\text{m}$ substrate is over-doped n^+ , covered with a thick layer of lightly doped n-type silicon. Strips of p^+ silicon at the surface are covered with aluminum tracks, which conduct the charge to the electrical read-out. A voltage around 80V is applied to the backplane, which fully depletes the n-type region and allows the collection of a minimum of $\sim 2.4 \times 10^4$ electron-hole pairs, for a normally incident minimum-ionizing particle (MIP).

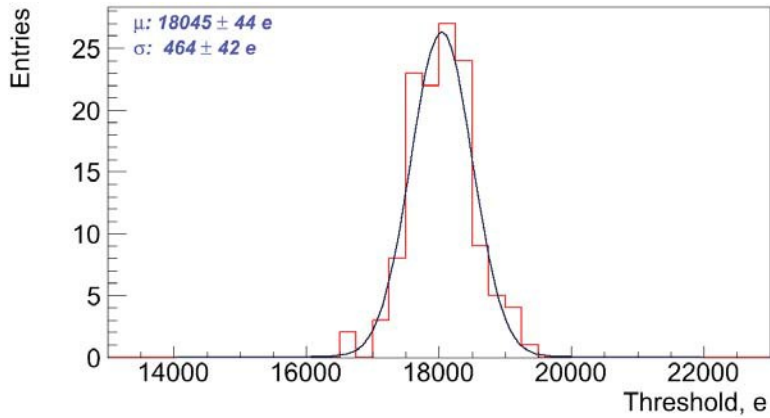


Figure 8. Example of the chip threshold dispersion measurement.

Measuring the analog response signal on the strips allows the determination of the input noise of the strips. One of the requirements of the silicon sensors is that the noise on the strips does not exceed 2000 electrons, which will guarantee noise occupancy on the silicon strips of less than 10^{-3} . The measurement of the input noise is also used to determine the total number of usable channels in the SVT, which is required to be greater than 99%. There is an allowance for bad channels during production. This is specified to be 1%, or five channels per module. As several bad channels in a row would reduce the sensitivity to multiple hits, a limit of four consecutive bad channels is applied.

2.4.1 Reconstruction of the analog strip response

Since the SVT modules are designed with a binary readout system, the analog channel

response cannot be measured directly. Instead, the analog response is reconstructed by injecting a calibration charge on the channel and measuring the corresponding occupancy over a range of threshold values. The calibration charge is produced by the charge injection circuitry of the readout chip.

The injected charge is shaped and amplified in the analog circuitry to form an output signal. The discriminator threshold determines whether or not the output signal corresponded to a hit. The probability that the injected charge produces a hit depends on the setting of the discriminator threshold. The average hit probability is measured by repeating the process of injecting charges and counting the fraction of readout triggers that produced a hit. This measurement is repeated over a range of threshold settings to produce an occupancy plot. The occupancy plot represents the probability p that a channel registers a hit at certain threshold voltage V_{thr} , given by:

$$p(V_{thr}) = \int_{V_{thr}}^{\infty} f(s)ds$$

where $f(s)$ is the probability distribution function that gives the chance of measuring a signal with a signal height s . The signal height distribution is assumed to be Gaussian:

$$f(s) = \frac{1}{\sigma_s \sqrt{2\pi}} e^{-(s-\mu_s)^2/2\sigma_s^2}$$

where μ_s is the mean signal height and the width of the Gaussian σ_s is the RMS noise of the signal. In between the high and low threshold regions, the occupancy curve is described by an error function, or S-curve (see figure 3), which can be fitted to the occupancy histogram for each channel, producing a mean value (discriminator threshold) and standard deviation (noise). Recording about 1000 events per threshold setting allows the appropriate mean and sigma to be extracted. By fitting the S-curve, the data acquisition software can determine the ENC of the module. Problem channels, such as where the fit fails, are tagged with defects and the generated data are placed in the database.

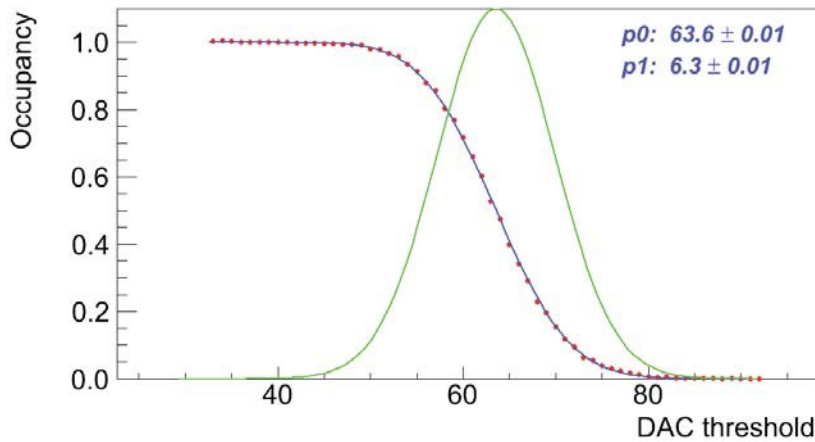


Figure 9. Typical example of an S-curve (red dots) as measured on SVT channel. The corresponding erfc fit (blue line) and signal response shape (green) as a function of signal height are also presented.

During the analog tests, S-curves are measured for all the chip channels over a range of

values for the injected charge (Figure 9, Figure 10). The threshold setting at which the probability of getting a hit is 50%, corresponding to μ_s , is **defined as the V_{t50} -point**. The value of the V_{t50} -point for each channel should increase linearly with the value of the injected charge, while the output noise, σ_s , is expected to be approximately constant as a function of charge. In practice, the output noise of each channel on the module is determined as the value of σ_s from the S-curve, obtained with a 3 fC input charge. The scans with no charge injection are also part of the module characterization sequence.

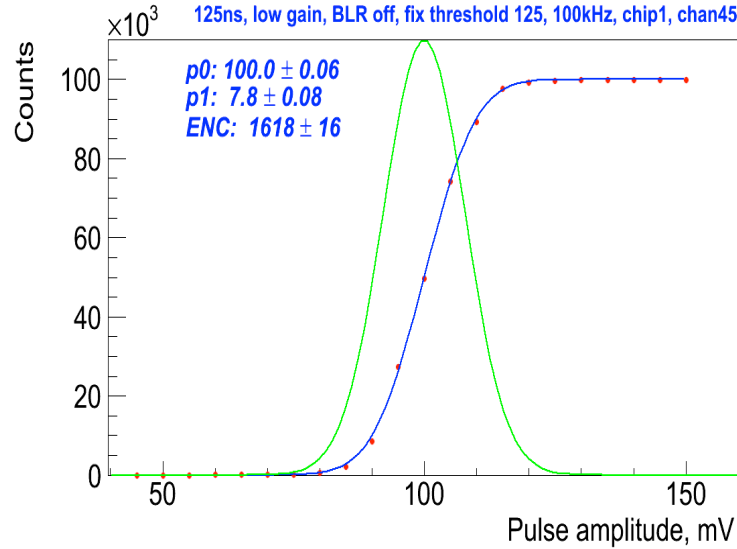


Figure 10. S-curve (red dots) measured with a fixed hit/no hit discriminator threshold and varying the amplitude of the injected calibration pulse. The corresponding erf fit (blue line) and signal response shape (green) as a function of signal height are also presented.

2.4.2 Noise and gain measurement

The S-curves that are measured for each SVT channel determine the output noise on the signal. By measuring the gain of the analog signal amplification, the input noise of each channel can be determined. The input noise can be used to identify several channel defects and helps to determine if the module is properly biased.

Response Curve: performs a 10-point gain scan. These data are then used to generate a response function, which maps injected charge to discriminator threshold (Figure 11).

Three Point Gain Test: the gain is determined for each chip by measuring S-curves at three different values of the injected charge: 3 fC, 4 fC, and 5 fC. One thousand events are sent for each bin and the range of threshold values is chosen according to the size of the injection charge. The gain (in mV/fC) then follows from the slope of a linear fit to the three V_{t50} -points as shown in Figure 12. It is used to measure the noise of a module and the similarity of response across the channels of a module. The output noise of each channel divided by the gain-factor of the chip results in the measured value of the input noise.

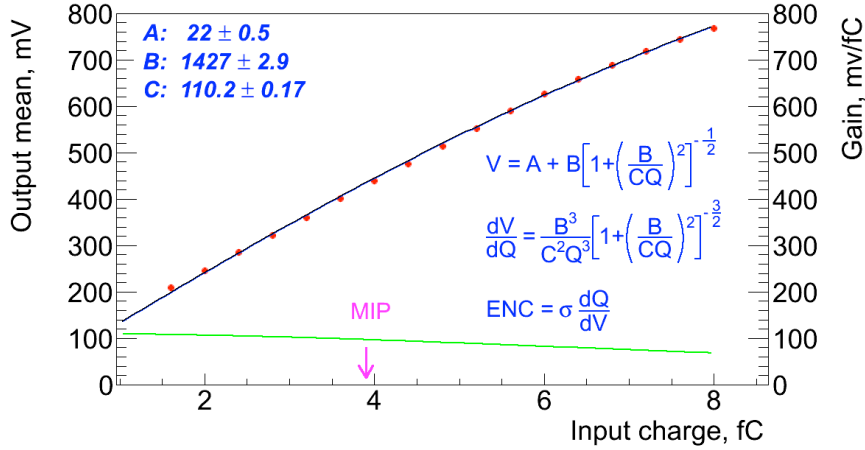


Figure 11. Response curve of the FSSR2 channel. Data (red) are fitted with a function (black) and gain is calculated at every point (green). Charge corresponding to the MIP is also shown.

Similar to the chip gain, to measure the channel gain, for each channel, a straight line is fitted to the mean and sigma parameters from the three scans in the test. The gradient of the slope represents the gain of the front-end amplifier at this point. This is used to translate the noise recorded at the output of the amplifier to that seen on the input. The onset of the straight-line fit is also recorded. Channels with too much noise are tagged as defective.

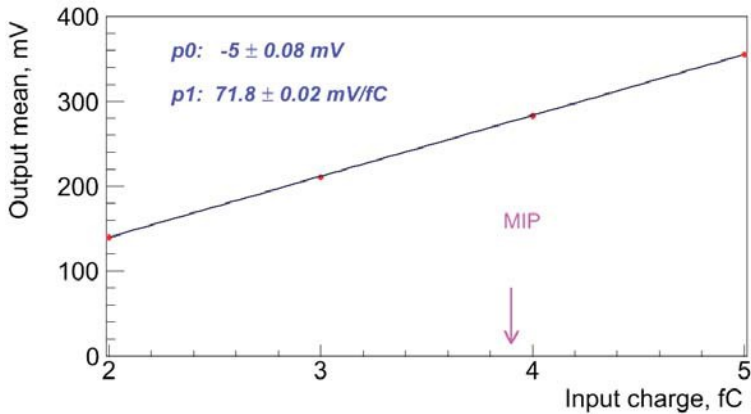


Figure 12. Example of fit to determine gain (in mV/fC) from measurements of the V_{t50} -points at four different values of the input charge. The V_{t50} -points represent the average value for all channels on the readout chip.

A summary of this data is recorded which includes the mean values per chip of the gain, offset, output noise, and input noise. Also recorded are the parameters for each chip of the straight line fit. During the calibration, a dedicated controller monitors the test results and when they are available, updates the configuration with the response curve parameters and masks channels that were recorded as defective.

One of the largest contributions to gain variation in the readout system is the chip-to-chip variation of gain. Changes in the chip LV or environmental temperature can also affect the gain of the readout channel. The response of all detector channels can be further equalized during offline reconstruction by correcting the signal magnitude by the

normalization factor. This procedure will be verified in further studies due to low granularity (3 bit) of FSSR2 Flash ADCs. Figure 13 shows the calibration plot for the flash ADC. Figure 14 shows gain dispersion in one of the chips of the module.

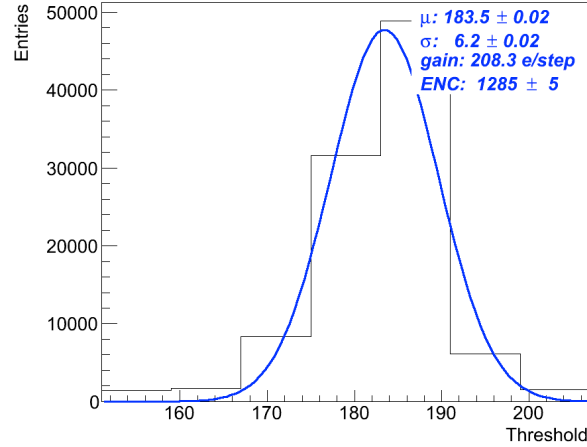


Figure 13. Flash ADC calibration.

The Calibration Client Graphical User Interface (GUI) monitors all of the information and stores and displays a view of selected data, for instance the noise figures for all of the connected modules, in a color-coded diagram.

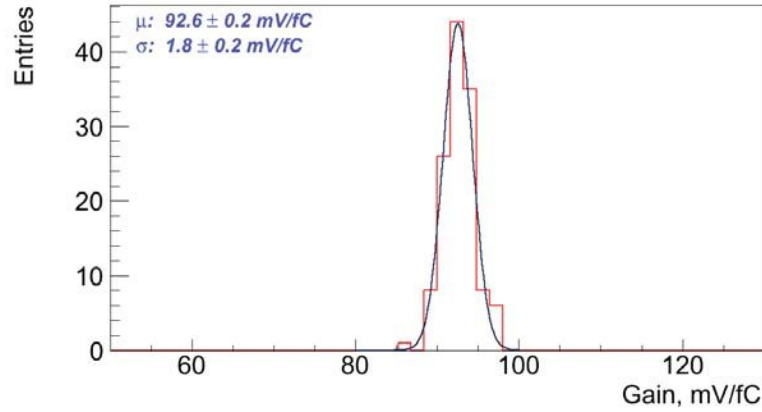


Figure 14. Example of the channel gain dispersion measurement.

From the measurement of the input noise, several channel defects can be identified. The main channel defects are defined as:

- **Dead:** measured input noise = 0, no hits are measured at any threshold for any injected charge.
- **Un-bonded:** measured input noise is < 800 e, most likely as a result of a broken bond between the FSSR2 and the first silicon strip sensor or the pitch adapter.
- **Partially bonded:** measured input noise is < 1500 e, a result of a broken bond between the daisy-chained silicon sensors (the threshold depends on the strip length of the tested channel).

- **Noisy:** the input noise is greater than 1.15 times the average input noise of all channels on the same chip.
- **Hot:** the input noise is greater than 1.25 times the average input noise of all channels on the same chip (the thresholds are defined experimentally).

The assumptions made for the input noise of partially bonded and un-bonded channels are based on the fact that the capacitive load on the channel is decreased when the silicon strip sensor is removed from the readout chain, resulting in a lower noise contribution, typically around 1000–1500 e.

The input noise also depends on the temperature of the silicon. The sensor temperature typically varies between modules and depends on the settings of the cooling used during the test. In the region of module temperatures during the assembly tests, the temperature dependence of the input noise can be approximated by a linear function. The slopes of the straight-line fits can be used to apply a temperature correction to the average measured input noise on each module, so that all results for the input noise correspond to a hybrid temperature of 25°C.

Noise Occupancy Test: one scan (occupancy histogram, see Figure 15) with no charge injection to find the noise value. This probes the tail of the noise distribution, which can show effects, which are masked by the higher occupancy at low thresholds. It also provides a crosscheck of the noise value obtained from the response curve measurement.

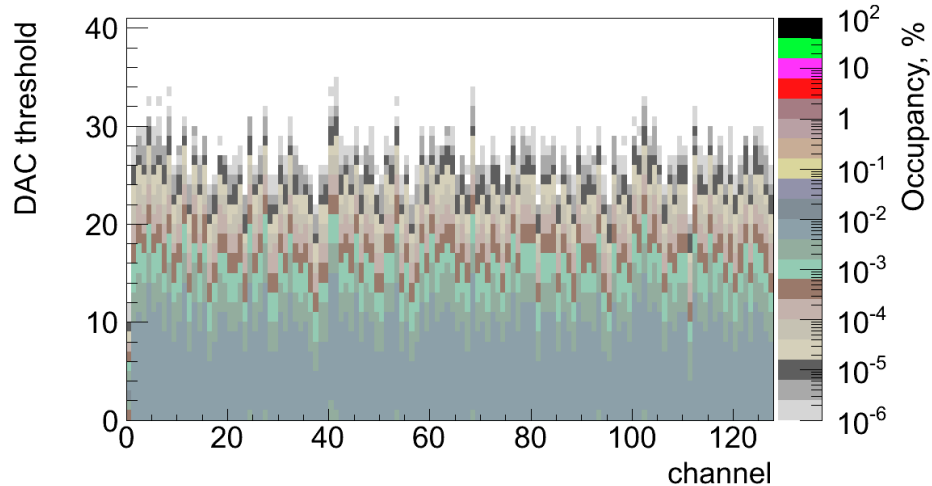


Figure 15. Channel noise occupancy vs. DAC hit/no-hit threshold (in DAC bins, One DAC bin corresponds to 3.5 mV).

It is important to ensure that the input noise of the modules does not increase with services successively added to the system, as that would indicate problems in the grounding scheme and common-mode noise has been introduced into the system.

2.4.2.1 Calibration of the detector channel noise

The noise and threshold dispersion constants for each individual detector channel must be measured, as these values are used by the zero-suppression algorithms implemented in the core logic of the FSSR2 and by calibration procedures to identify defective channels.

Noise is measured using external, low frequency calibration charge injected in the absence of signal. Longer silicon strips have higher capacitance and thus a higher expected value for the input noise. Noise calibration should account for the different strip lengths and pitch adapter layouts that affect the input capacitance of the preamplifier. Threshold dispersion is defined to be the standard deviation of the distribution of means obtained from the parameters of the complementary Erf fit as described in section 2.4.1. Fitting the mean noise versus silicon strip length, the following parameterization is obtained:

$$\text{Noise (e)} = A + B \times \text{length (cm)},$$

which should be compatible with the measurements performed during the SVT integration period, prior to installation.

Figure 16 shows examples of the input noise measured for the 256 channels of the top side of the pre-production module. One can notice the channels with open inputs and noisy strips. These defects are identified during module QA procedure.

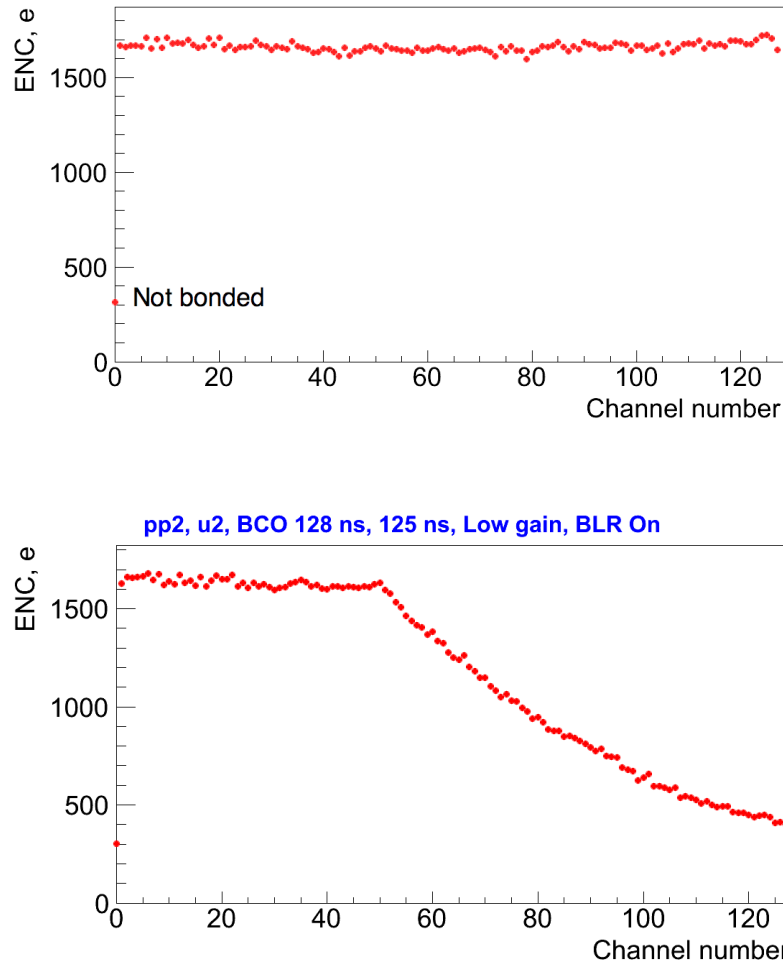


Figure 16. Example of the input noise measured on the top side of the SVT module. First readout chip (top plot) is connected to the longest strips (~33 cm) while part of the second chip (bottom plot) is wire bonded to the shorter strips due to variable pitch design of the sensors.

The average noise in these two chips is below 2000 electrons which is typical value for the module. The expected value of the input noise depends on the length of the silicon strips as shown in Figure 17.

The individual sources of noise on the detector module can be identified and measured by plotting the ratio of the minimum to the median noise value for each FSSR2. The ratio takes advantage of the fact that broken wire bonds on the detector modules effectively reduce the input capacitance to individual channels of the FSSR2 chips. Broken wire bonds can occur between (in ascending order of capacitance): the FSSR2 and pitch adapter, the pitch adapter and silicon sensor, and between the sensors. Fitting to these populations, corresponding to the previous broken wire configurations provides an estimate of different noise contributions.

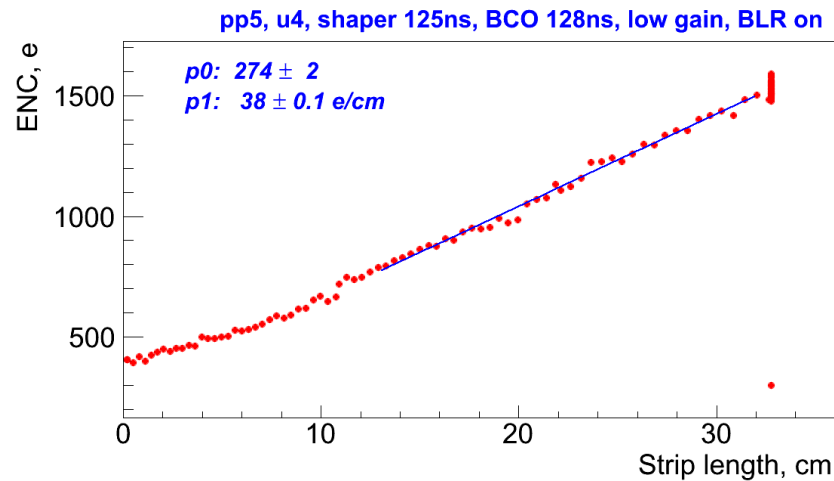


Figure 17. Input noise versus strip length showing the straight line fit as expected from the linear dependence of the channel noise on the preamplifier capacitive load.

2.4.2.2 Calibration with γ source

An absolute calibration of gain and noise using a radioactive source of Am²⁴¹ with intensity of 1 mCi has been performed (Figure 18). Americium has γ peak at the energy of 59.5 keV, corresponding to ~ 16436 e⁻ in silicon.



Figure 18. Setup for absolute calibration with Americium γ source mounted on a hybrid sensor.

A sliding window approach has been used to measure the spectrum. The hit/no-hit threshold and one of the thresholds of flash ADCs were set to define the window. It's bin

size was set to 1 DAC bin (3.5 mV). The random trigger from external pulser was used to define the time intervals at each threshold step in a sliding window scan. The number of noise hits has been verified to be negligible using the same acquisition time.

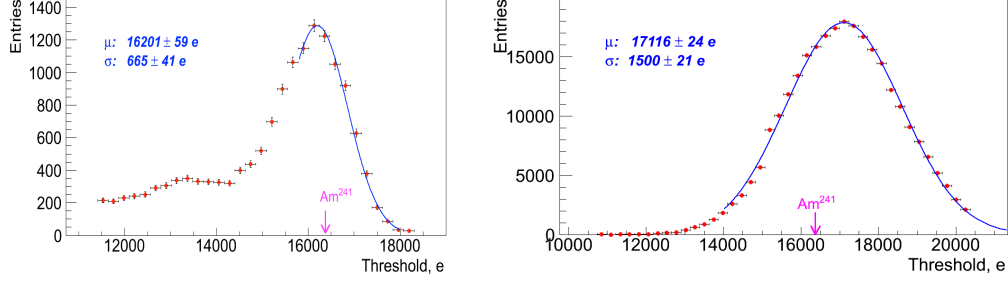


Figure 19. Spectrum of Am^{241} expressed in keV (left). Spectrum of external pulser with amplitude set to 66 mV corresponding to energy deposition of 59.5 keV (right). Arrow indicates expected position of the peak.

Americium peak has been compared with the spectrum of the external pulser with amplitude set to the same energy as the Am^{241} γ emission. Figure 19 shows the Am^{241} spectrum in keV and a typical spectrum of the external pulser. The σ of the Gaussian fit is comparable with noise measured with a threshold scan. The mean values of the Gaussian fit to the Americium spectrum and to the external pulser spectrum are comparable within measurement uncertainties. The absolute calibration performed with γ source is consistent with calibration performed with external pulse generator, considering a nominal value for the inject capacitance of 40 fF. Measurements were done using the Far and Hybrid sensors of the module. Far sensor peak within 1.6 % of the calibration peak from external pulser with amplitude 66 mV corresponding to the charge deposited in the sensor by Am^{241} . Hybrid sensor peak is within 1 % of the calibration peak from external pulser.

2.4.2.3 Signal measurements with β source

A measurement of signal with Sr^{90} β source has been performed using the similar approach and setup as in calibration with Am^{241} γ source. The difference was related to the higher strip multiplicity which caused changes in measurement procedure and in data analysis (using clustering algorithm to account for charge sharing among adjacent strips). The hit/no-hit threshold and six out of seven thresholds of flash ADCs were set to define equal sized bins. The last bin of the flash ADC contains overflows. The highest bin without overflows has been used as a sliding window. It's bin size were 1 DAC bin (3.5 mV) and 5 DAC bins. The lower bins were used to get information on the pulse height of the channels adjacent to the seed strip. The hit/no-hit threshold was fixed while the size of the higher bins (except the one used for sliding window) increased each time the window moved to the higher thresholds. The measured spectra are presented in Figure 20 and are compatible with expected position of energy loss from a Minimum Ionising Particle (MIP).

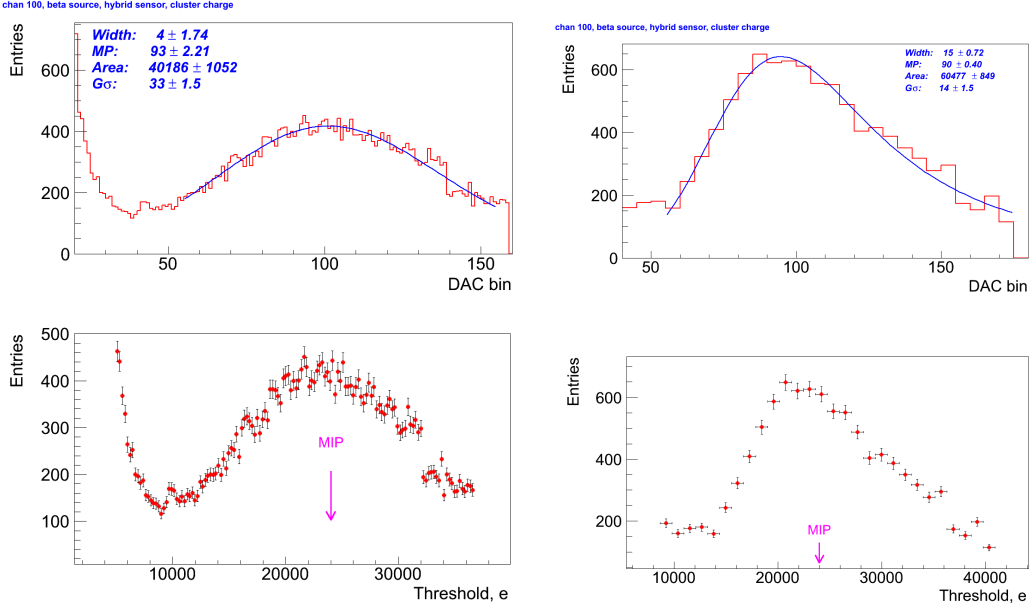


Figure 20. Spectrum of Sr^{90} expressed in DAC bins (top) and in keV (bottom). Left and right spectra present the sliding window scans taken with different window and threshold sizes. Arrow indicates expected position of the most probable value for the MIP.

2.5 Burn-in test

The burn-in test is the last step in the QA procedure at FNAL before a module is sent to JLAB. The group of modules is run for 24-72 hours at a temperature of around 37°C . Clocks are sent continuously with a brief confirmation test performed at regular intervals. This provides a burn-in check and the status monitored for any time- and temperature-dependent defects.

2.6 Module problem summary

2.6.1 Defective channels results

The number of channel defects found per module by measuring the input noise on the modules, is reported and recorded in the SVT conditions database, separated into the different types of channel defects. The data collected during module production, JLAB reception tests, SVT assembly, and final commissioning are analyzed to verify that no significant change in the number of channel defects is found between the different test stages. From the defective channel results, the percentage of operational channels is calculated.

3 SVT configuration, conditions, and alignment databases

The configuration database stores the configurations of all the modules, VME cards, crates, and power supplies in the system. This is used extensively by the SVT Application Programming Interface (API) to find which cards are in each crate and which modules are connected to which card. The GUI also uses the configuration to find out where each

module is placed.

The power supply configuration for the LV is stored in the firmware of the power supply module. For the HV power supplies the configuration is set remotely by the software. Configuration is transferred to the Detector Control System (DCS) system outside of a run to save time when the parameters do not change.

The bulk of the configuration needed by the SVT API is the parameters required to set up each module. The configuration database also stores mappings of modules between different naming schemes for use by the user interface.

The data which are stored in the MySQL database are: gain, noise, threshold dispersion, module location, bad channels, PS modules, crates, cables, slow controls, DAQ, results of mechanical surveys, alignment constants, etc.

Conditions DB monitoring should allow at least three levels of details to monitor:

1. Monitor the status of all the DBs, accounts and tags used
2. For a given DB/account/tag retrieve trend profiles of a given CondObject using the Historic Data Quality Monitor (HDQM) architecture and the DQM GUI
3. For a given run, retrieve and navigate the full info contained in the CondObj, summaries should be written in specific tables of the Historic DQM, to be easily accessible in the step 2

4 SVT commissioning during tracker assembling

4.1 ***Module construction***

This section covers topics related to the fabrication of the tracker. The necessary activities are hierarchical and require careful staging. In the initial phase various components are procured, tested and pre-assembled. Examples of these components are the detectors, pitch adapters, front end chips, backing structures, and hybrids. Other examples would include fabrication of cables, power supplies, and cooling system components. The staging of these activities is critical for the SVT construction milestones to be met. In recognition of this, the SVT construction and assembly process is being designed and scheduled within the overall SVT project plan and managed by the 12 GeV Upgrade Group.

Over the period leading to the publication of this document, the SVT group went through a series of design reviews which culminated in the selection of various baseline technologies to be used in the tracker. The SVT development team has produced engineering specifications and designs for the various components. The construction program must ensure that all these components are properly handled during assembly in an environment, which will ensure good performance and long-term reliability of the tracker.

The first, most critical, and largest task in the construction sequence is the assembly of the silicon detector modules at the Silicon Detector Facility (SiDet, Fermilab). An important aspect of the module assembly process is ensuring that all modules are built the same way. Each module for the SVT is expected to be identical. This is desirable for a number of reasons, in particular it is an effective way to maintain the same quality, the

use and fabrication of materials and fixtures may be optimized with the elimination of wasteful duplication.



Figure 21. One of the SVT prototyping modules showing the test hybrid attached to three daisy chained CMS Tracker Outer Barrel silicon sensors.

In this section a brief description of the issues related to module construction and barrel assembling processes is given. The SVT team is in a good position to accurately specify these processes based on significant prototyping work (Figure 21, Figure 22) and a broad background of experience coming from previous experiments. SVT collaborators have worked on silicon trackers for LHC and TeVatron experiments. A detailed description of the actual assembly process can be found in the SVT TDR.

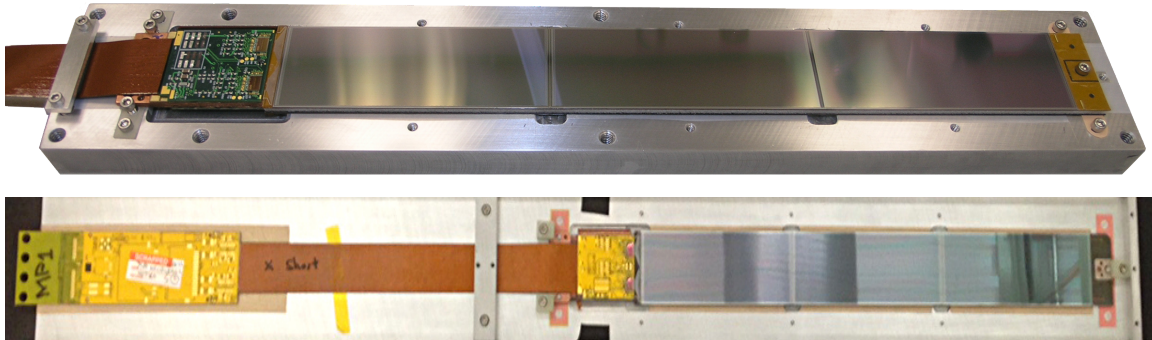


Figure 22. SVT pre-production module (in wire bonding fixture) showing the top side of the rigid-flex hybrid attached to three daisy chained SVT first article silicon sensors assembled at Fermilab's Silicon Detector Facility (top). Pre-production module in the carrier box (bottom).

While the module design process is aimed particularly at achieving certain performance specifications (noise, temperature gradients, etc.), it is clear that another set of issues exist which go beyond the module design itself. Assembly procedures, quality control methods, production tests, application of adhesives are examples of items which impact more on the manufacturing aspect of this process than the physical choice of the module configuration. It is the purpose of the construction process design to focus on these issues of module manufacturing. A range of prototyping activities has been undertaken as part of defining the procedure. The result of this activity is as follows:

- module construction specifications have been adopted
- a set of working principles have been adopted
- the module assembly process flow has been specified
- a baseline mechanical assembly process has been designed in detail

- the costs and necessary infrastructure are understood.
- testing procedures have been specified
- production capacity and workload for the SiDet has been specified
- technical issues for study have been identified

The aim of the module construction process is to supply the modules, including spares, for the SVT barrel. The schedule is specified in the SVT project plan. Production is scheduled to begin in spring 2013, during which year all production modules will need to be delivered and assembled into the barrel.

4.2 Barrel assembly

The precision needed during construction is determined by physics requirements. The overall requirements are listed in Table 1 of the SVT TDR. As construction moves from the relatively small scale of module construction to overall detector assembly it becomes increasingly difficult to control mechanical tolerances. The precision available with modern mechanical fixturing and metrology is exploited in the module assembly to allow most of the available error to be assigned to the overall assembly steps.

A uniform database to track materials and modules has been selected and user interface is being designed.

Modules are mounted on the barrel (Figure 23) using techniques designed to accomplish the task with minimal risk to the modules. This requires the design and manufacture of tooling to allow the SVT modules to be mounted onto the support structure, as well as the development of procedures to fasten down the modules and attach the services. At the start of the build, all layer modules are mounted in groups; the group is tested to check for module damage during the assembly procedure and then module mounting is resumed with the addition of more modules, after which the layer is tested again. By iterating the processes of mounting and testing, no net additional defects should be introduced during the assembly process.

Module mounting begins with the preparation of a list of selected modules for each layer, using the performance parameters obtained during module testing at FNAL. The selected modules are moved to storage near the module mounting station.

The thermal requirements dictate that the amount of thermal grease making the cooling contact between the modules and their cooling blocks be carefully controlled. This is achieved using a precision liquid dispenser and a syringe. Thermal grease DC340, manufactured by Dow Corning, is applied to the main-point blocks using a 10-dot pattern. The mass of grease applied is adjusted by varying the air pressure and air pulse duration on the dispenser. The mass of grease dispensed is checked before a group of five or six modules is mounted by applying grease to the sample block. The typical grease coverage over a block is checked by mounting a clear plastic plate on the sample block and applying the torque used for module mounting.

The SVT is mounted in a frame, which allows the SVT to be positioned at precisely the right angle so that the mounting points for all modules could be brought to exactly the same position relative to the module mounting jigs, and strain relief for the cables. Modules are then extracted from their carrier boxes before being located on to the support

structure pins using the module-mounting jig. Miniature CCD cameras are used to view the relative positions of the module's precision mounting holes with the corresponding pins on the cooling blocks to allow the operator to correctly position the module before it is slid on using the grabber. The module is released from the grabber and the module-mounting jig is withdrawn. A torque driver is used for the final tightening.

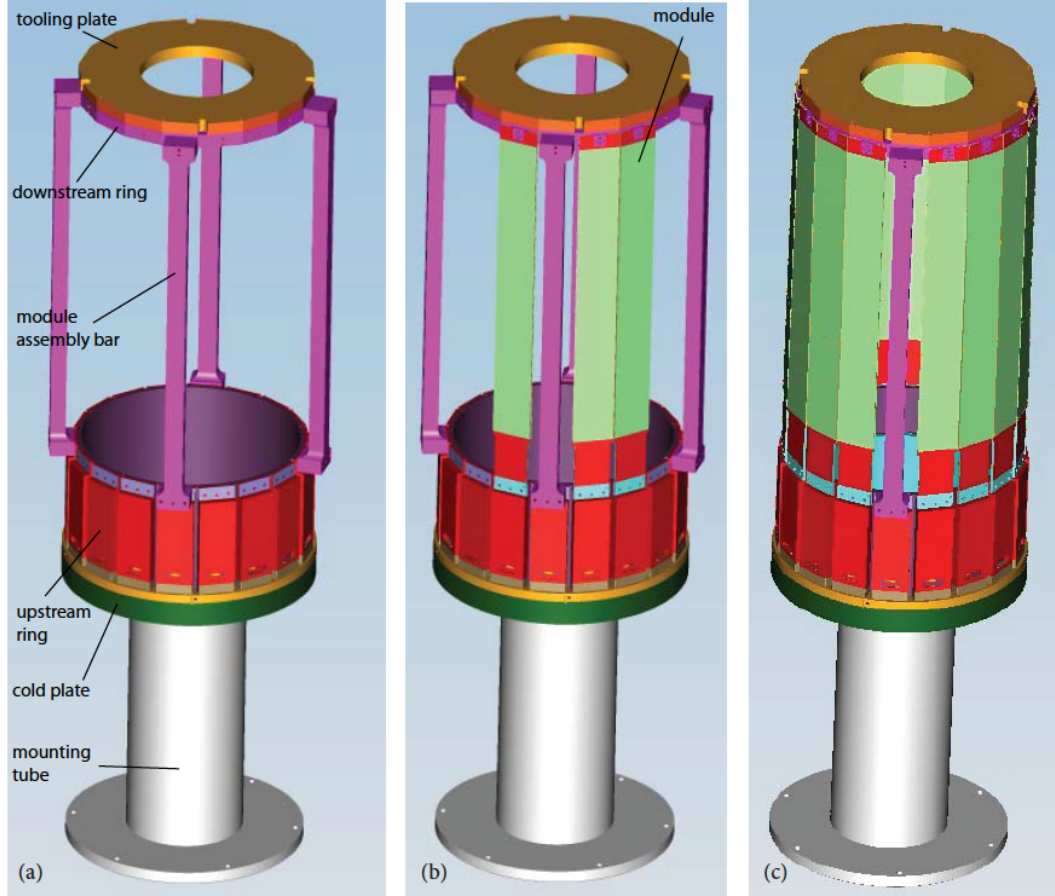


Figure 23. SVT barrel assembling.

As a final check, the distance between the mounting pins is measured. The positions in the plane of all of the mounting pins relative to the reference holes in the barrel are measured on a CMM with a precision of $10\text{ }\mu\text{m}$ and incorporated into the alignment database to provide an initial estimate of the position of each module on a barrel. The alignment accuracy should be comparable for all layers of modules; however the specifications are tightest for the inner layers.

4.3 Readout hardware configurations

SVT assembly is carried out at JLAB in the SVT clean room in the EEL building. An important part of the assembly procedure is the exercise of the electrical functionality of the module, by running appropriate tests to check continued operation. This is an important reason for the development of the SVT DAQ software, which should be tested

in different hardware configurations, starting from small systems and extending to a complete barrel.

All readout hardware configurations in the SVT clean room are read out through 3 VME crates, which is enough to read out the whole barrel. Four module configurations are used as part of the development for the full barrel tests: a two-module system for small-scale tests, a larger test system based on part of a barrel, and the full barrel.

4.3.1 Two module configuration

A simple module set-up is used during software development and for reception of modules from FNAL. This consists of two boxed SVT modules on a desk, VME crate with VME Silicon Controller Module (VSCM) card (

Figure 4, Figure 24), LV/HV PS in MPOD crate, and linux/OS X PC. The final version of the electrical harness used to provide power and data links to the modules, but the modules are contained in the same carrier boxes used for electrical testing during production and transportation. These allow chilled water to pass close to the module cooling plate to keep the modules from overheating and provide support for the modules, as the barrel is not available. The final SVT power supplies are used, with a full-length cable to a dedicated MPOD crate.



Figure 24. SVT readout VSCM module with two data cables in the VME crate.

4.3.2 Configuration of test sector

This configuration is designed for the system tests, commissioning of the cooling system and other services, and for cosmic ray tests. The sector or part of the barrel region is fitted with modules. The barrel sector allows testing and development of the software system for use with larger numbers of modules than possible with the carrier box setup. The sector provides the first use of the DCS - DAQ Communication system to transfer DCS data to the DAQ. This allows current information about the modules to be stored with the results from tests. It also allows for future integration, such that the DAQ may respond to events such as loss of bias on a module in a controlled manner. This enables a test of all the hardware and software reading out real modules to check for any adverse effects before being used on the full barrel system.

4.3.3 Configuration for barrel

The final configuration is the full barrel during assembly. Modules to be mounted on the barrel receive a quick reception test using SVT DAQ before they are mounted onto the barrel. Modules are mounted in stages and electrically tested before the next set is added. The barrel is tested in a specially constructed light-tight screen. The testing is done at room temperature operation with careful control of the humidity within the room precluding casual access.

The power cable connections for the assembly are the same as for the final system. Using the final power supplies requires the use of the appropriate connectors. The noise behavior of the barrel during assembly is directly comparable to the final system.

Noise figures are expected to provide a reasonable indication of performance in Hall B. Power supply currents and voltages are checked and the data path is checked using an analysis based on the raw data.

During mounting, the modules are tested using a cut-down version of the characterization sequence: the mask test, three-point gain, and noise occupancy. Once mounted, longer tests are run on the complete barrel. These include the addition of the Double Trigger Noise and Synchronous Trigger Noise tests. The Synchronous Trigger Noise test is the only test carried out where all modules receive a trigger at the same time. All the other tests use triggers generated independently on individual modules.

4.4 Noise measurements

Noise is one of the critical parameters, which will affect the physics performance of the SVT. Though a direct comparison to the specification is not possible, due to the differences in the noise environments, the measurements can be used to verify uniformity and to pick out modules with problems. Noise can be measured in two ways: interpolated from the noise measurements in the threshold scans using the calculated gain, or from the noise occupancy measurements at different thresholds. A fundamental difference between these two methods is the presence of the injection charge in the threshold measurements. Additionally, the two analysis methods make different assumptions about the structure of the noise and of the front-end amplifier response curve at different threshold levels. The "noise" value is the input noise value calculated from the response curve test. The "noise occupancy" plots show the noise value calculated from the noise occupancy test.

4.4.1 Measurement of common mode noise

Common mode noise refers to a variation of the signal, which affects groups of channels in a coherent way. It can be caused by a common electromagnetic pick-up, noise on the supply voltage, etc. It adds to the noise and can eventually even create artificial hit patterns. The susceptibility to common mode noise depends both on the individual detector module and on the system environment. The spectrum of the common mode noise is a priori unknown. Most difficult is the detection of Gaussian common mode noise. In an analogue read-out scheme, the common mode contribution can be measured on an event-by-event basis. For a group of channels, the pedestals are subtracted from the raw signals and channels with real hits are excluded. Then the average signal seen on the channels is a good approximation to the common mode noise contribution, as the single

channel random noise cancels to a large extent (depending on the number of channels in the group). This common mode contribution can be subtracted from the signals. Common mode is of particular concern in digital read-out systems as it cannot be measured on an event-by-event basis and therefore a correction for common mode is impossible. It can only be estimated on a statistical basis, analyzing some sample of events. Therefore, it is vital for a digital system to have negligible common mode noise. This calls for methods to detect and measure coherent effects, which can then be used in the system evaluation and optimization.

4.4.1.1 Excess noise

If the single channel random noise is well known, the common mode noise can be detected as excess noise. This method requires a very reliable understanding of the expected single channel random noise and it is not sensitive to the coherence of common mode. Therefore, this is at best a very indirect measure of common mode noise.

4.4.1.2 Log (occupancy) vs. (threshold)²

If the intrinsic noise in a system is purely Gaussian, and in the absence of other noise sources, the probability p of surpassing a threshold τ is given by the complementary error function:

$$p(\tau) = \frac{1}{2} \operatorname{erfc}\left(\frac{\tau}{\sqrt{2}}\right)$$

For thresholds much larger than the single channel random noise ($\tau \gg 1$), this probability can be approximated by:

$$\begin{aligned} p(\tau) &\approx -\frac{1}{\sqrt{2\pi\tau}} \exp\left(-\frac{\tau^2}{2}\right) \\ \ln(p) &\approx -\frac{1}{2}\tau^2 - \ln(\sqrt{2\pi\tau}) \end{aligned}$$

using the asymptotic series for the complementary error function. This is already a good approximation for $\tau > 1.5$; leading to the conclusion that purely Gaussian noise should give a straight line in the plot of the logarithm of the occupancy vs. the square of the threshold over much of the useful range.

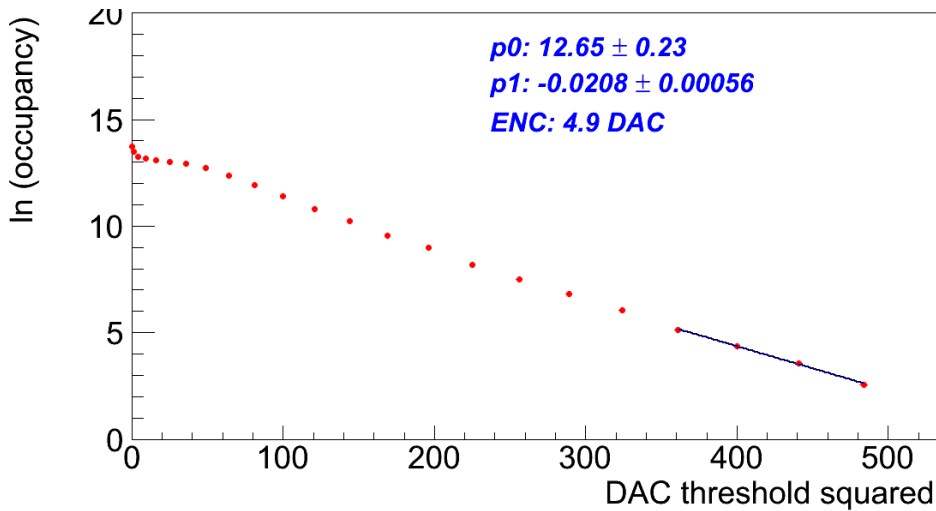


Figure 25. Log of noise occupancy as a function threshold squared as measured on a single channel of the SVT module.

Occupancy refers to the (normalized) total number of hits in all channels in a run. The power of this plot is to show non-Gaussian noise contributions as deviations from this linear fall-off. Gaussian noise contributions, on the other hand, just change the slope of the linear fall-off. A good knowledge of the expected single channel random noise is needed if further conclusions about Gaussian common mode are to be drawn. This method also cannot distinguish between correlated and uncorrelated noise. Therefore it is not suitable to detect Gaussian common mode noise. Figure 25 shows this plot for a single channel of the SVT module.

4.4.1.3 Raw data plot

The most basic display of the data is a plot in which the hit map is plotted in the plane spanned by channel number and event number. This plot is extremely useful in understanding the data quality as it shows immediately

- dead/noisy/sick channels;
- channel occupancy;
- uniformity across the channels;
- uniformity across the events in a run;
- coherent effects on the channels in individual events.

The hit maps for the top and bottom sides of the module are built at 50% occupancy. Common mode noise is observed in the form of horizontal bands in the hit map. Although this plot does not provide quantitative results, it is clearly an important diagnostic tool.

4.4.1.4 Occupancy per event plots

A correlated noise detection code builds a histogram of the hit strip count for each chip, called the OPE (occupancy per event) histogram. This provides information on the structure of the events in an occupancy histogram. If the hits are evenly distributed among all the events, then each event will have a small number of hits. Correlated noise

manifests itself by inducing a large number of hits in a single event, which can otherwise be masked by the evenly distributed noise. An analysis of these histograms is based on looking for unexpected channel hit counts.

Common mode noise should lead to a large number of hits in some events and very few in others, compared with the expectation from the single channel random noise.

Therefore, the distribution of the number of hits in an event N_e should be a measure of coherent noise. While the distribution is narrow without common mode noise, it widens strongly when common mode noise is present. One can calculate the width of the N_e distribution which is expected in the absence of common mode noise. In this case, N_e has to follow a binomial distribution, $\text{Bin}(N_e; n, p(\tau))$ for n channels and a hit probability $p(\tau)$ for the given threshold τ . The mean number of hits is then

$$\overline{N_e} = \sum_{N_e=0}^n N_e \text{Bin}(N_e; n, p(\tau)) = np(\tau)$$

Thus, the probability p can be approximated by the observed mean number of hits per event divided by the number of channels n , and for the variance of the N_e distribution

$$\text{Var}(N_e) = np(1 - p) = \overline{N_e}(1 - \frac{\overline{N_e}}{n}).$$

Therefore, the expected standard deviation can be calculated from the observed average number of hits per event, without further assumptions. If the observed distribution is wider, one can conclude that coherent noise is present. In a real system, large channel-to-channel variations of the channel occupancy may be present, resulting for instance from large channel-to-channel threshold variations. These variations in general do not widen the N_e distribution. In the absence of common mode noise and for equal mean number of hits in all channels, the largest standard deviation is obtained for $\overline{N_e} = n/2$. A smaller or larger $\overline{N_e}$ leads to a more narrow distribution, according to the above formula. The N_e for a mixture of channels with different occupancies is the sum of values taken from narrow distributions and the resulting distribution itself is narrow. If the observed $\overline{N_e}$ is close to $n/2$ and the channel occupancies vary, then the standard deviation calculated with the above formula is an overestimate. Therefore, a data distribution wider than this calculated standard deviation still indicates common mode noise.

In order to derive a measure for the common mode noise contribution, one has to calculate the mean and the variance of the N_e distribution in the presence of common mode noise. The effect of a shift of the signal by a common mode noise contribution is equivalent to shifting the threshold by the same amount, but in the opposite direction. Therefore, one can implement the effect of common mode noise by choosing the threshold τ in each event from a probability distribution $g(\tau)$. For the case of Gaussian common mode noise it is given by

$$g(\tau) = \frac{1}{s\sqrt{2\pi}} \exp\left(-\frac{(\tau - \tau_0)^2}{2s^2}\right)$$

where s is the standard deviation of the common mode noise in units of the single channel random noise σ , and τ_0 is the original threshold. The distribution of the number of hits per event N_e is then a superposition of binomial distributions for varying thresholds.

At the 50% point:

$$s^2 = \frac{\sin(\alpha)}{1 - \sin(\alpha)} \text{ with } \alpha \equiv 2\pi \frac{\text{Var}(N_e) - (n/4)}{n(n-1)}$$

If the mean occupancy of the channels is 50%, then the common mode noise can be calculated from the observed mean and variance of the distribution of the number of hits per event using this equation.

A useful generalization of this formula is found by identifying the $n/4$ term with the binomial variance of N_e at the 50% point. The observable Γ defined as

$$\begin{aligned} \Gamma^2 &\equiv \frac{\sin(\tilde{\alpha})}{1 - \sin(\tilde{\alpha})} \text{ with} \\ \tilde{\alpha} &\equiv 2\pi \frac{\text{Var}(N_e) - \bar{N}_e(1 - (\bar{N}_e/n))}{n(n-1)} \end{aligned}$$

In the absence of common mode noise, Γ is zero no matter how many channels there are or how the threshold is set. Γ increases strongly for increasing common mode noise. The strongest effect is observed for zero threshold, i.e. at the 50% point. In this case, by definition, the quantity Γ approximates the ratio of common mode noise over single channel random noise:

$$\text{common mode noise} \approx \Gamma \times \text{single channel random noise for } \bar{N}_e \approx n/2.$$

The effect of channel-to-channel threshold variations is weak. The N_e plot and the observable Γ are very sensitive to common mode noise. In addition, this method is highly specific to the coherence as any kind of single channel random noise does not broaden the N_e distribution.

The occupancy per event distributions can be used to study common mode noise on all chips of the HFCB. If there is more coherent noise on the chip (or the bottom side vs. top side), the distribution of occupancy per event is wider. Nonuniform noise across the chips would result in several peaks in this distribution. Under the influence of coherent noise, the occupancy per event distribution no longer follows binomial statistics, therefore, the observable Γ has to be used to measure the common mode noise contribution.

At 50% occupancy Γ is a linear function of common mode noise. In presence of a fixed amount of common mode noise, the Γ versus occupancy follows nearly a parabolic shape. For a measured Γ value, common mode noise can be calculated for different occupancies using the fit for this distribution. Γ is symmetric about 50% occupancy. A good fit of Γ as a function of occupancy and common mode noise is given by

$$\bar{\Gamma} = \left(\frac{\text{Common Mode Noise}}{\text{Single channel random noise}} \right) \left(1 - \frac{(|0.5 - \text{Occupancy}|)^{2.15}}{0.25} \right)$$

This parametrization can be solved for the common mode noise contribution and can be used to estimate the common mode noise contribution from the measured Γ i.e.

$$\frac{\text{Common Mode Noise}}{\text{Single channel random noise}} \approx \frac{\Gamma}{(1 - 4 \times (|0.5 - \text{Occupancy}|))^{2.15}}$$

The statistical error on this common mode noise measurement comes only from the error on Γ , neglecting the error on the occupancy. The error on Γ^2 can be calculated using standard error propagation formulae and is given by,

$$\sigma_{\Gamma^2}^2 = \left(\frac{d\Gamma^2}{d\bar{N}_e} \right)^2 \sigma_{\bar{N}_e}^2 + \left(\frac{d\Gamma^2}{dVar(N_e)} \right)^2 \sigma_{Var(N_e)}^2; \text{ with}$$

$$\frac{d\Gamma^2}{d\bar{N}_e} = \frac{2\pi}{n(n-1)} \left(\frac{2\bar{N}_e}{n} - 1 \right) \left(\frac{\cos(\tilde{\alpha})}{[1 - \sin(\tilde{\alpha})]^2} \right)$$

$$\frac{d\Gamma^2}{dVar(N_e)} = \frac{2\pi}{n(n-1)} \left(\frac{\cos(\tilde{\alpha})}{[1 - \sin(\tilde{\alpha})]^2} \right)$$

In the absence of common mode noise N_e follows binomial statistics and therefore errors on mean and variance of N_e in this equation are given by,

$$\sigma_{\bar{N}_e}^2 = \frac{\sigma^2}{N}$$

$$\sigma_{Var(N_e)}^2 = \frac{1}{N} \left(\sigma^2 \left(1 + 3\bar{N}_e - \frac{3\bar{N}_e^2}{n} \right) - \sigma^4 \right) \text{ with}$$

$$\sigma^2 = np(1-p) = Var(N_e)$$

where N denotes the total number of events and is assumed to be large.

In the presence of common mode noise, the error on mean and variance can be found using Gaussian approximation and are given by,

$$\sigma_{\bar{N}_e}^2 = \frac{\sigma^2}{N}$$

$$\sigma_{Var(N_e)}^2 = \frac{2\sigma^4}{N} \text{ with}$$

$$\sigma^2 = \langle N_e^2 \rangle - \langle N_e \rangle^2 = Var(N_e)$$

The error on Γ can be found by propagating the error on Γ^2 by,

$$\sigma_\Gamma = \frac{1}{2\Gamma} \sigma_{\Gamma^2}$$

Finally the error in the measurement of common mode noise is given by,

$$\sigma_{CMN} = \frac{a}{\sqrt{N}} \times \frac{2\pi\sigma}{2n(n-1)\Gamma} \times \left\{ \frac{\cos(\tilde{\alpha})}{(1 - \sin(\tilde{\alpha}))^2} \right\} \times \left\{ \left(\frac{2\bar{N}_e}{n} - 1 \right)^2 + 2\sigma^2 \right\}^{\frac{1}{2}} \text{ with}$$

$$a = \frac{1}{(1 - 4 \times (|0.5 - Occupancy|)^{2.15})}$$

Γ is calculated for runs with different number of events and various values of common mode noise. For lower number of events per run Γ has larger statistical uncertainties which flatten for large numbers of events per run. This analysis shows that at least 500 events per run are needed for the statistical uncertainty to be less than 5%.

The occupancy per event for the top and bottom sides of the module are built at 50% occupancy. The shape of the distribution is studied and occupancy variation from chip to chip is examined.

Γ method predicts how the common mode noise σ_C normalized to random noise σ_R varies with the measured Γ and occupancy. However, intrinsic random noise will generally be

unknown, as only the total noise σ_T , containing random and common mode noise sources can be measured. Since the common mode noise adds in quadrature to random noise, $\sigma_T^2 = \sigma_C^2 + \sigma_R^2$, we get,

$$\sigma_C^2 = \frac{\sigma_T^2 a^2 \Gamma^2}{1 + a^2 \Gamma^2}$$

The common mode noise contribution can be calculated from the measured Γ at a given occupancy (threshold) and total noise σ_T , where the total noise σ_T is measured from the S-curve for every channel of each of the four chips on the module and the results are averaged by chip. Results from different chips are compared. Another useful tool is to plot the average common mode noise on the module as a function of occupancy. To generate this plot the threshold is varied in steps.

4.4.1.5 Correlation matrix

The most detailed information on the correlation between the signals from different channels is obtained from the correlation matrix. If we consider two channels x and y then the correlation between them is

$$cor_{xy} = \frac{\langle xy \rangle - \langle x \rangle \langle y \rangle}{\sigma_x \sigma_y}$$

The standard deviation is

$$\sigma_x = \sqrt{\langle x^2 \rangle - \langle x \rangle^2} = \sqrt{\langle x \rangle - \langle x \rangle^2}$$

(similarly for y) as for the binary data $x_i=x_i^2$. $\langle x \rangle$ is the occupancy in channel x (Ω_x) and $\langle xy \rangle$ corresponds to the occupancy of a hypothetical channel representing the logical AND of the channels x and y ($\Omega_{x,y}$) for the correlation of channels x and y

$$cor_{xy} = \frac{\Omega_{x,y} - \Omega_x \Omega_y}{\sqrt{\Omega_x - (\Omega_x)^2} \sqrt{\Omega_y - (\Omega_y)^2}}$$

with

$$\begin{aligned}\Omega_x &= \frac{\text{number of events with a hit in channel } x}{\text{total number of events}} \\ \Omega_y &= \frac{\text{number of events with a hit in channel } y}{\text{total number of events}} \\ \Omega_{x,y} &= \frac{\text{number of events with a hit in channels } x \text{ and } y}{\text{total number of events}}\end{aligned}$$

Calculating this quantity for all pairs of channels results in the full correlation matrix. In the absence of coherent noise (and for infinite statistics), the correlation cor_{xy} of two channels vanishes, no matter what the occupancy of the two individual channels is. Common mode noise will most likely lead to a positive correlation. In addition to the detection and quantification of common mode noise, the correlation matrix provides information about the range of coherence. If common mode effects are bound, for instance, to each read-out chip and there are several chips in the system, the matrix will show square regions of non-zero correlation. Higher level of coherent noise would result in higher correlation among the chips. If the common mode is due to some cross talk between channels, the correlation matrix will show a band structure around the diagonal.

4.4.1.6 Autocorrelation

Autocorrelation is a powerful technique used in signal processing applications for revealing hidden periodicities in apparently random noise. It is normally applied by multiplying the received signal by a copy of itself which is shifted in time. For our purposes, we are looking for channel correlations rather than time correlations, and we shall define a discrete form of the autocorrelation function as

$$A(m) = \sum_{i=1}^n x_i x_{(i+m) \bmod n}$$

where n is the number of channels, and x_i is the signal in the i th channel, defined so that a ‘hit’ has a numerical value +1 and a ‘zero’ has value -1. Channels which are shifted beyond n are ‘wrapped around’ using the mod function. The resulting function, $A(m)$ is the autocorrelogram for a given event. At the 50% threshold (zero, in this case) and without correlated noise, the time averaged value for $A(m)$ is

$$A_0(m) = \begin{cases} n & \text{for } m = 0 \\ 0 & \text{otherwise} \end{cases}$$

At other values of the threshold, the autocorrelogram may be calculated by considering the expectation value for the variable $x_i x_j$ ($i \neq j$). Given that the two are independent and obey Gaussian statistics, the average value is

$$\overline{x_i x_{j \neq i}} = (1 - 2p)^2 = \operatorname{erf}^2\left(\frac{\tau}{\sqrt{2}}\right)$$

The effect of common mode noise is to effectively change the threshold about its mean value across all the channels.

$$\overline{x_i x_{j \neq i}} = \frac{1}{s\sqrt{2\pi}} \int_{-\infty}^{\infty} \exp\left(-\frac{(\tau - \tau_0)^2}{2s^2}\right) \operatorname{erf}^2\left(\frac{\tau}{\sqrt{2}}\right) d\tau$$

where s is the common mode standard deviation and the common mode noise is assumed to be Gaussian. This function is most sensitive to common mode noise when $\tau_0=0$, for which the integral has the closed form

$$\overline{x_i x_{j \neq i}} = \frac{2}{\pi} \tan^{-1}\left(\frac{s^2}{\sqrt{1+2s^2}}\right)$$

For small values of common mode noise, the function erf^2 may be replaced by its Maclaurin expansion around $\tau_0=0$, which yields

$$\overline{x_i x_{j \neq i}} \approx \frac{2}{\pi} s^2 \approx 0.64s^2$$

4.4.1.7 Comparison of the methods

Table 1 summarizes the features of the different methods considered. As the first two methods are not specific to coherence, they are only useful if there is huge extra noise in the system or if this extra noise is non-Gaussian. For a basic understanding of the data quality, the raw data plot is very useful and provides qualitative information on coherent effects. The observable Γ , derived from the standard deviation of the number of hits per event, yields a quantitative estimate of the common mode noise and is computationally fairly simple to achieve, given that the normal diagnostics for a binary system include

occupancy statistics in any case. It is very sensitive and specific to the coherence of common mode noise. The correlation matrix provides, in addition, detailed information about the range of coherent effects, as well as the strength of the correlation for each pair of channels. Similar information is obtained by the autocorrelation method.

In the SVT microstrip detector system currently under construction, noise analysis has to deal with dozens of detector modules and tens of thousands of channels. Here it should be useful to quantify coherent noise on the module level by a single number, for instance the Γ variable, which will allow to survey all modules and identify problematic areas. Noise which is coherent between modules and bigger parts of the system can be assessed by combining channels into bigger units like chips or modules and using the number of hits in these units as input for the raw data plot or the correlation matrix.

Method	specific to coherence	sensitive to common mode non-Gaussian	Gaussian	range of coherence
excess noise	no	no	no	no
$\log(\text{occ.}) vs. \text{thresh.}^2$	no	yes	no	no
raw data plot	yes	yes	yes	yes
occupancy per event	yes	yes	yes	no
correlation matrix	yes	yes	yes	yes
autocorrelation	yes	yes	yes	yes

Table 1. Comparison of the methods

To test the described methods common mode noise is created by injecting a 10 MHz signal of amplitude 0.5 V. The signal injection is done by putting the output cable from the signal pulse generator underneath the module inside the module carrier box. The cable acts as an antenna emitting a radio frequency. Results with and without the signal injection are compared to see the difference and usefulness of the common mode noise methods described here.

4.4.2 Closely separated triggers

The Double Trigger Noise tests are designed to look for effects of pick-up between closely spaced triggered events. The test works by scanning the delay between two triggers while reading out and histogramming only the second event. The mean occupancy of each chip in a single module is plotted as a function of the delay between triggers.

4.4.3 Synchronous trigger test

The final test run on the barrel is an occupancy measurement using triggers sent synchronously to the whole barrel. A series of triggers are sent to the modules at a rate of 100 kHz. Every N^{th} event is histogrammed. This is a restriction due to the event bandwidth in DAQ. The noise values are recorded from a run of synchronous triggers at a threshold of 1 fC. All of the modules should have mean noise occupancy well below the specified 10^{-3} .

4.5 Calibration procedure

4.5.1 Scan production

The main function of the SVT DAQ during calibration is to produce occupancy histograms for analysis by the higher-level SVT DAQ software, known as scans. The main parameters to describe a scan are:

- the configuration variable that is to change over the course of the scan
- the values the configuration variable should take
- the sequence of commands, known collectively as a trigger, sent to the modules for each event
- the number of triggers to send
- which modules will send events to the DAQ

A scan can also have some options, which change the behavior of the scan process, for instance, whether the calibration line is in use. Once complete, a scan is identified to the SVT DAQ software by the run number, a scan number within the run and the serial number of the module.

Many calibration histograms have occupancies many times higher than that observed during a physics run. As the length of the bit-stream generated by the FSSR2 chip is in general proportional to the hit occupancy, then so is the time taken to read out the chip. This means that the module cannot be read out at full speed and the trigger speed must either be slow enough to allow the readout of the maximum bit-stream length, or it must vary according to the actual occupancy recorded by the module during the scan.

The standard scan provides a histogram of the occupancy on a module as the threshold is varied. This is normally carried out with a particular amount of charge injected. Many other scans are possible by modifying the various parameters on the scans. The following gives examples of some of these scans and how they make use of different features.

Configuration Check: A special scan, based on the probe scan, can be used to check the configuration of the connections between modules. This can then be compared to the configuration found in the database.

Noise Occupancy: A final characterization test, the Noise Occupancy test scans thresholds around the nominal 1 fC threshold, with no charge injection, and measures the occupancy, see Figure 26. To measure the (lowest) occupancy at high thresholds, of the order of a million events are sent to the modules. At low thresholds and high occupancies recording this many events takes a prohibitive amount of time, therefore the number is reduced. The histogram code is constrained to send a constant number of triggers for each threshold setting. To send different numbers of events to different bins in the histogram, the procedure is repeated starting at a different bin each time. The first round puts the lowest number of events in all the bins. Subsequent repetitions accumulate more events in the later bins until all the requested events have been sent.

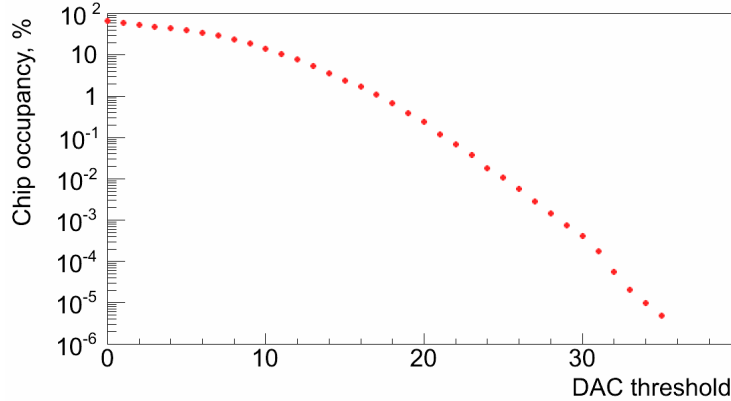


Figure 26. FSSR2 chip occupancy vs. DAC hit/no-hit threshold measured on the SVT module.

4.5.2 Fitting service

Once the histograms have been produced by the SVT DAQ and published to the event data server, they are ready for analysis. The first stage is to make fits to the data for each channel. The Fitting Service monitors the event data server for new histograms. When a histogram appears, a selection is made based on the configuration variable being scanned over. Once the fit has been made, the results are published to another data server.

4.5.3 Analysis service

Analyses are produced in a similar manner to fits, but data for all channels in a module are taken account of. The data server with test control data from the Calibration Controller is monitored along with the data servers for both event data and fitted data. Once the appropriate data is available the analysis can be performed.

Each test is analyzed by a separate class, which registers interest in the name of the test as reported by the Calibration Controller data. The result of the analysis of a test is a series of numbers describing the high level behavior of a module. The GUI can display this in various ways. For instance after a three-point gain test, the analysis produces information on the gain, onset, and noise for each channel. These can be displayed in channel-by-channel graphs for each module. Alternatively, the data can be summarized to produce a report in the same format as SVT DAQ uploads to the production database. This data is then used by the GUI to summarize the results for many modules, color-coding the graphical representation of the barrel. Finally, data from the analysis is used by the Calibration Controller to update the configuration of each module.

4.5.4 Archiving service

The data servers store data that is produced online. The data is lost when the programs no longer run. The Archiving Service is responsible for saving the data to persistent storage. It monitors the data servers that the other services place data on to. This is then serialized and stored permanently on disk with regular backups.

4.5.5 Module indexing schemes

During the module production phase, the primary scheme used for tests is the module serial number. This is used to index all the tests in the production database. For assembly

and for the final experiment, this single address is not enough. The DAQ system needs to be able to look up a configuration in the production database, control the correct module and receive data from it, request changes in the power supply parameters from the DCS system, and also allow a geographical visualization of the modules on the barrel. A module channel in the DCS system can be referenced by the crate and the channel in the crate. The barrel geography (the position of a module on the barrel) can be described by the region on the barrel and a position along the region.

All the information for the configuration service is stored in XML. This allows different types of structured information to be stored together. The configuration can then be arranged on the file system in a more user-friendly way, for instance by using one file for each module configuration. A utility program enables the XML file corresponding to a module to be downloaded from the production database.

4.6 SVT commissioning and cosmic ray tests

The VME-based SVT DAQ software is used to test the performance of a small number of modules before mounting them onto the support structure at JLAB’s barrel assembly site. As regards the software implementation, each VME card should have a library in SVT DAQ, which represents the interface to the remainder of the software and uses VME drivers to talk to the card. On top of this is built a system for sending bursts of triggers, changing the module configuration appropriately and collecting the resulting histograms.

Each test in the characterization sequence is controlled by a ROOT script, which is able to access the high level library. This results in an occupancy histogram, called a scan, which corresponds to the scan variable and trigger selection requested. An appropriate function is fitted to each channel under control of a second ROOT script, which then analyzes the resulting data to produce the results in a form appropriate to each test. The results take the form of a set of summary plots and summary data, which are uploaded to the production database so they may be reviewed later.

This system works for small numbers of modules (Figure 27). For larger numbers, as in barrel assembly and in the final experiment, a large number of crates is needed. This requires coordination between the computers connected to the VME bus and controlling the cards, particularly important during calibration scans. Another limitation of SVT DAQ is in the fitting of the histograms, which is one of the slowest parts of the analysis process and is carried out on the controlling computer. These limitations must be addressed in the final SVT DAQ system.

From the start of SVT assembly onwards, the readout of the SVT modules is carried out using the final SVT DAQ system instead of that based on the SVT module test DAQ. Much of the remaining code in SVT DAQ will control histogram creation and the building of the configuration streams to be sent to the modules. Additionally, the fitting of histograms and the analysis of tests for only a few modules in SVT DAQ consumes a substantial amount of resources. To scale to larger numbers of modules, these tasks should be offloaded. For use beyond assembly, the system must be capable of coordinating between multiple VME crates. For these reasons, instead of retrofitting the SVT module test DAQ program, a new structure should be developed, while making use of the knowledge gained from development of SVT module test DAQ.

In common with SVT module test DAQ, the final SVT DAQ software must be able to:

- Configure modules according to an external specification
- Produce histograms of scans across module variables
- Fit different functions to the histograms
- Analyze data to produce new configuration parameters and defect lists
- Replicate the analysis carried out by SVT module test DAQ
- Provide access to low-level functionality for expert users
- Scale to all modules
- Make use of CLAS12-provided software to facilitate future interaction with other sub-detectors
- Communicate run state with the Detector Control and Safety system

For the SVT stand-alone cosmic ray test, a group of modules representing about 20% of all SVT modules are cabled to make “top” and “bottom” sectors in azimuthal angle, ϕ . There is no applied magnetic field and care is taken to reproduce, as far as possible, the service routing and grounding of the final setup in Hall B. All data are taken with module temperatures sensors at approximately 25°C using portable chiller.

Cosmic rays are triggered using coincident signals from scintillators located above and below the barrel. The resultant hit data are transferred by the SVT DAQ, written to disk, and analyzed offline. As well as using the cosmic trigger, noise data are recorded in physics mode under a variety of test conditions, using fixed frequency or random triggers.

To time-in the SVT with the cosmic trigger, the modules’ relative timings are calculated from known differences in cable lengths. The global delay is determined using dedicated monitoring histograms which record, as a function of the global delay, the number of coincident hits on neighboring chips on opposing sides of each module. After timing-in, hits from cosmic rays traversing the SVT can be observed on the online event display.

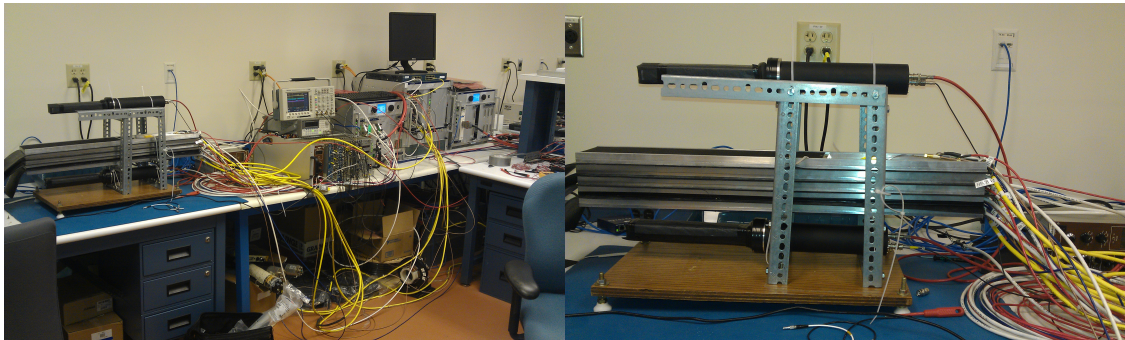


Figure 27. Test stand for commissioning the SVT modules with cosmic rays.

The number of cosmic ray events and noise events is defined based on the results of MC simulations. The average noise occupancy is measured and should be below the 10^{-3} specification. The distribution of noise hits per event should be described by a Gaussian curve so there is no evidence of correlated noise. By contrast, events triggered by cosmic rays should have a long tail showing the expected correlated hits.

With one threshold in the electronics, only the efficiency of detecting signals above the threshold in a single strip can be obtained at a time. Extraction of analogue information

from the binary electronic read-out is accomplished by performing efficiency vs. threshold curves, which give the integral of the pulse height spectrum. The following parameters are determined: the efficiency at a fixed threshold of 1 fC, the median of the pulse height spectrum, i.e. the 50% efficiency point, and the most probable pulse height in the pulse height spectrum, obtained from the threshold curve by differentiation. By scanning the thresholds, the pulse height (Landau) distribution is obtained in its integral form, convoluted with a Gaussian with a width characteristic of the system. The median of the Landau distribution is the threshold of 50% efficiency. In order to get the threshold, a modified error function is fitted to the efficiency data,

$$eff(q) = p_3 \left(1 - erf \left(\frac{q - p_1}{p_2} f(q) \right) \right)$$

where

$$f(q) = max \left(0.6, 1 - p_4 \left(\frac{q - p_1}{p_2} \right) \right)$$

The function, erf , is the integral of the Gaussian distribution. The function, $f(q)$, is a phenomenological correction function to modify the Gaussian to the Landau distribution. The fitting parameters expressed the median ($p1$), the width ($p2$), the saturation ($p3$), and the skew ($p4$).

4.7 Beam tests with SVT modules

Measurement and verification of the tracking performance of the SVT module in test beams is part of the process of commissioning of the silicon tracker. Tests are performed to explore the module performance under various operating conditions including bias voltage, magnetic field, incidence angle etc. A particular emphasis is given to understanding of the operational consequences of the binary readout scheme and data-driven architecture of the FSSR2 chip.



Figure 28. Test module used for proton beam test in Protvino.

4.7.1 Beam test goals

The goals for the SVT beam test are:

- Validation of the SVT detector module
- DAQ testing (event builder, time synchronization, readout up to 6 readout lines, event rate)
- Measurement of Signal-to-Noise Ratio (S.N.R.)
- Measurement of cross-talk between the two sides and two modules
- Measurement of hit efficiency vs. threshold
- Measurement of noise occupancy vs. threshold

- Measurement of Charge Collection Efficiency (C.C.E.) vs. bias voltage
- Data taking in different running conditions (bias voltage, LV, threshold, BLR on/off, shaping time, low/high gain, BCO clock, trigger rate, readout frequency)
- Gain calibration using Flash ADC
- Measurement of position resolution
- Measurement of efficiency along the module length, near the edges of the silicon wafers
- Measurement of channel inefficiency: study of defective (dead, noisy, broken bonds) channels and strips
- Study of the response of the detectors when hit near or on strips which have various kinds of defects
- Measurement of capacitive coupling and strip multiplicity
- Measurement of the Lorentz angle
- Testing cluster finding algorithms
- Testing alignment algorithms
- Validation of the SVT reconstruction code (local reconstruction and tracking)

4.7.2 Test setups

Performance of the SVT modules has been measured in beam tests throughout their development. In 2011 a prototype module has been studied with 50 GeV proton beam in Protvino (Figure 28). In 2012 two SVT pre-production modules were used in beam test at JLAB running parasitically behind the Heavy Photon Search (HPS) silicon tracker.

Figure 29 shows the setup used for commissioning of two SVT modules during the beam test in Hall B (May 2012). Another beam test is scheduled for 2013 with production grade modules using precise beam telescope and magnetic field. The effect of a strong magnetic field is tested by inserting the complete setup in the superconducting magnet. The magnet provides a vertical field over a volume large enough to contain the entire assembly. The modules are mounted with strips almost parallel to the field and normal to the incident beam, emulating the configuration of the modules in the barrel. The deviation of the charge carriers due to the Lorentz effect is studied in detail yielding a precise measurement of the Lorentz angle.



Figure 29. Commissioning of the SVT modules during beam test in Hall B.

4.7.3 Beam telescope

A typical arrangement for this test consists of a scintillator trigger, a beam telescope and environmental chamber containing the modules under test. The telescope and modules under test are mounted on a granite table sitting on a trolley on a set of rails permitting insertion into the active volume of the magnet. Telescope and DUTs are placed on a customized motorized table with remote control. Two scintillator detectors sensed by photo-multiplier tubes are used to detect the passage of beam particles and trigger the readout system. Triggers can originate from different sources: external (beam scintillators) and based on a hit multiplicity on each layer side. The trigger signal timing jitter is on the order of few nanoseconds. The acceptance of the scintillators is about $2 \times 2 \text{ cm}^2$, large enough to contain typical beam spots and comparable in size to the acceptance of the beam telescope. As the SVT modules have a sensitive area around $4 \times 11 \text{ cm}^2$ only a small region is tested at any one position of the module in the beam.

A beam telescope is used to measure the trajectories of beam particles independently of the devices under test. The telescope modules consist of two perpendicular silicon micro-strip sensors providing an X-Y space point. The sensors should have a strip pitch about $50\text{-}60 \mu\text{m}$ and are read out by the same DAQ as the tested modules. The modules are rigidly mounted on the same massive granite table as the modules under test, two before and two after the environment chamber. A spatial resolution on the order of $5 \mu\text{m}$ is expected in this configuration. In case pre-existing telescope modules with readout chips other than FSSR2 are used and shaping time is different from the modules under test, to ensure that the track detected in the telescope corresponds in time with the SVT modules, one of them is also used to provide a reference hit. This “anchor” module does not undergo threshold or bias scans but is kept at constant settings selected for high efficiency and low noise occupancy. The requirement that the anchor module records a hit matching the telescope track also effectively eliminates residual inefficiencies due to clock and readout glitches, and since it is located among the modules under test, helps eliminate badly reconstructed or widely scattered tracks.

A beam test typically consists of a large number of short runs during which the front-end discriminator threshold is scanned in steps through the expected signal range, resulting in an efficiency “s-curve” from which the collected charge distribution can be recovered. The runs of the threshold scan are repeated for each combination of the operating parameters of interest such as the silicon sensor bias voltage, the applied magnetic field, the angle of incidence on the silicon, the trigger timing, the position of the beam around the module, and the operating modes of the FSSR2.

A full characterization of the module front-end parameters such as gain and noise is made using the FSSR2's in-built calibration circuit in situ prior to the beam test under the same conditions as for the beam measurements to avoid setup effects. For example, the temperature and humidity differences of the chips may have a few percent effect on the noise measurement.

4.7.4 Cooling

The modules under test are mounted in a light-tight, thermally insulating chamber. The chamber is flushed with cold nitrogen gas to ensure a dry atmosphere. Each of the modules is contained in its own aluminum test box with heat sink to which it is thermally coupled through its designed cooling contact surfaces. The test boxes are cooled by water chilled to around 15°C. Each module dissipates up to 2 W power. The resulting temperatures, measured by sensors mounted on the electronics hybrid of the module, are monitored continuously. Modules have HV bias currents on the order of 2 μ A.

During the beam test, data from telescope modules and SVT test modules are assembled into events and written to data files. These raw data are processed by offline CLAS12 reconstruction software. Offline processing includes the internal alignment of telescope and module planes and the reconstruction of tracks with dedicated tracking algorithm using the measurements of the beam telescope.

4.7.5 Alignment

The beam telescope provides four very precise measurements in two perpendicular space coordinates. The reconstruction of the track and the interpolation to the plane of the module under test require a precise knowledge of the relative alignment of all detectors in the setup. The positions of telescope and SVT modules, though stable, are only approximately fixed by the mounting frames. A precision measurement of the relative alignment of all planes is obtained using the tracks in a large number (\sim 10000) of events. The alignment procedure minimizes the alignment error by iteratively varying the alignment parameters.

As a first step in the alignment procedure, the position of the global telescope frame is fixed by identifying X- and Y-axes with respectively the horizontal and vertical coordinates measured by the first telescope module, and the Z-axis with the beam direction. Once the global system is defined, the remaining telescope detectors are aligned by minimizing the distance of their hits to tracks reconstructed from the outer two modules. At this stage only two space points are used to define a track. Ambiguities due to noise hits are effectively avoided by rejecting events in which all four planes under consideration do not have exactly one hit. After the internal alignment of the telescope, full three or four space point information from the telescope can be used to reconstruct tracks projected through the modules under test. The alignment parameters of each of the

two planes of the test modules are varied until the difference between the interpolated track position and the measurement by the plane converges to a minimum. The two planes of each module are aligned independently.

When a magnetic field is applied, the tracks have a significant curvature. Moreover, the Lorentz effect leads to a displaced position measurement. For data taken in the magnetic field the alignment procedure described above - with straight tracks - is nevertheless applied. The effects of the magnetic field are thereby absorbed in the effective module positions. This procedure allows the interpolation of the track to the modules because all tracks have closely the same momentum. The alignment procedure is repeated each time the setup is physically accessed or whenever the magnetic field is changed.

4.7.6 Track reconstruction

The offline pre-processing of the data includes the reconstruction of the tracks using the space points measured by the telescope. The measurements of the two perpendicular planes of each telescope module are combined into three-dimensional space points. Track segments are constructed by combining the space points from the most upstream and most downstream modules. The track is then refined by including the space points from the intermediate telescope modules if the distance between the track and the space point is within 50 microns. Events are included if the track contains at least three space points after this cut.

A number of track quality indicators are available to select a sample of tracks with a predefined efficiency and purity. The most important are: the number of space points in the track fit, the χ^2 of the fit, the track gradients with respect to the beam axis, and whether a hit is recorded in the anchor module. The position where the tracks are incident on each module is interpolated from the telescope hits with a precision of approximately 5 μm including the alignment error. The dominant error is due to multiple scattering within the module array.

4.7.7 Event selection

A run consists of the order of 10,000 events collected under a fixed set of operating conditions including discriminator threshold. The first step in the analysis is the selection of the event sample. To select a sample of clean, unambiguous events, a number of selection criteria are applied:

- **Single track events.** In a small fraction of events (depending on the beam intensity, generally of the order of few percent) more than one track is reconstructed from the telescope information due to its relatively long shaping time. To avoid ambiguities, events with more than one telescope track are rejected from the analysis, as are events where no telescope track has been accepted.
- **Track quality.** From the remaining sample, only those events are accepted where the telescope track satisfies quality criteria. Most analyses require that the track quality criteria listed above be fulfilled. Moreover, a hit close to the track in the anchor module is required. This combination of cuts efficiently removes fake tracks and tracks suffering a large deflection due to multiple scattering. The loss of statistics in this stage depends on the values of the cut, but is in general of the order of 10-30%.
- **Masked channels.** During the characterization of the modules faulty channels, for

example dead, stuck or particularly noisy channels, are identified. These channels are configured to be masked in the FSSR2 chips so that they are never read out. Events in which the track points to one of these “bad” channels or their immediate neighbors are rejected from the analysis of that particular module. In modules passed QA the fraction of masked channels is below 1%. The loss of statistics in this step is therefore small.

- **Time window.** A final cut removes those events where the random trigger phase falls outside an optimum window. This window is optimized separately for each module to account for small cable length differences. In the beam tests the data output taken by the DAQ takes into account hit information from the preceding and succeeding BCO time bins as well as that centered on the trigger time to maximize the recorded information. The time window cut, however, requires a hit in the central time bin.

4.7.8 Efficiency and noise occupancy

The most important benchmarks for SVT binary module performance are the efficiency and the noise occupancy at the operating threshold, nominally 1 fC. A detector plane is considered efficient if a binary cluster center is located within 150 μm of the interpolated telescope track position. By definition, the efficiency of good strips is measured. The inefficiency due to dead sensor or electronics channels is not accounted for, nor is the inactive area between sensors. The maximum tolerable number of defective channels is defined in a separate specification. The noise occupancy is measured by counting all hits in special flagged events taken in the periods between accelerator spills, during which there is no beam occupancy. As these events are interleaved with beam events the operating conditions are identical. The noise occupancy is defined as the probability to find a hit due to noise in one channel in one clock cycle.

When the modules are operated with sufficient over-depletion, a long plateau where efficiencies over 99 % is expected. The noise occupancy, on the other hand, is a rapidly falling, nearly Gaussian, function of threshold, independent of bias voltages high enough to deplete the detector. The occupancies should coincide rather accurately with the expectation from the equivalent noise charges measured during the characterization of the module. By analyzing the plots of efficiency and noise occupancy taken at different thresholds the operating range can be found. The operating range is defined as the range in thresholds where the efficiency and noise occupancy specifications are both met.

In detectors with analogue readout the charge on multiple consecutive strips is measured and the position is determined from the properties of the cluster. The clustering procedure yields a quasi-continuous position measurement. In the binary readout scheme, however, the signal in most cases is over threshold on only one strip for tracks at normal incidence. Thus, only a discrete measurement is available. This could lead to non-uniformities in the response depending on the position of the track with respect to the two closest strips, particularly in the inter-strip region. FSSR2 chip has binary architecture with embedded 3-bit flash ADC for calibration purposes. Although not as precise as 8-bit ADC commonly found in the microvertex readout ASICs, this information can be accounted for in the track reconstruction algorithm for clusters with strip multiplicity higher than one.

The efficiency versus inter-strip position is studied for perpendicularly incident tracks.

The position is expressed in units of the read-out pitch: inter-strip position 0.5 corresponds to telescope tracks crossing the detector at equal distances from the two strips and inter-strip positions of 0 and 1 correspond to tracks that are incident on the center of the readout strip. In the central region diffusion of the charge carriers leads to increased charge sharing. The lower signal on each of the strips is reflected in the reduced efficiency at high threshold. However, at the operating threshold the efficiency is expected to be uniform over almost all interstrip positions. This distribution is smeared by the uncertainty in the position of the interpolated track that becomes significant at this level.

4.7.9 Spatial resolution

The spatial resolution is obtained as the width of the residual distribution - the distribution of the difference between the extrapolated track position and the center of cluster. Since the SVT sensors have graded pitch geometry, the residuals are rescaled by the ratio between the readout pitch and the local pitch to facilitate comparison. For single strip clusters residuals form a uniform distribution from $-p/2$ to $p/2$, where p is the readout pitch, characteristic for binary readout. The spatial resolution due to single-strip clusters is given by the RMS of a uniform distribution with a width equal to the pitch:

$\sigma = p/\sqrt{12} \sim 45 \mu\text{m}$ (at the hybrid end of the sensor). As the multi-strip clusters predominantly occur in a narrow region in the central region between two strips the resolution of the multi-strip clusters is better than that of single-strip clusters. The residuals distributions are smeared by the uncertainty on the interpolation of the telescope tracks. For tracks of normal incidence the fraction of multi-strip clusters is expected to be small and the resolution is close to $45 \mu\text{m}$, independent of the operating parameters.

The residual distribution provides a measurement of the spatial resolution of a single detector plane. The stereo angle between the two detector planes of the SVT module allows the determination of a two dimensional space point. The intersection of two $156 \mu\text{m}$ wide strips defines a rhombus with short axis $\frac{p}{\cos \alpha/2}$ and long axis $\frac{p}{\sin \alpha/2}$, where p is the readout pitch and α is the stereo angle. The short axis corresponds to the X-axis of the global coordinate system in the test beam, while the long axis is identified with the Y axis. Projecting the uniform distribution in the rhomb on both axes yields the distributions that are fitted with Gaussians to get the spatial resolutions in X and Y.

The squared position resolution $\sim 1/E^2$. In this plot the contribution of multiple scattering shows up as a linear behavior and the intrinsic resolution corresponds to the intercept at the origin (i.e. for infinite momentum particles). At fixed track incidence angle Θ (angle in the plane parallel to the strips) the data have a larger slope and a smaller intercept compared to the results for zero degrees. The larger slope can be attributed to the increase in the material of a factor $1/\cos \Theta$. In addition, the higher signal to noise ratio obtained at larger angles can produce a better intrinsic resolution.

4.7.10 Median charge

In the binary readout scheme, it is necessary to scan the discriminator threshold through the charge distribution in order to reconstruct the full signal distribution. The curve of efficiency as a function of threshold, the “s-curve”, measures the integrated charge distribution. The collected charge distribution is described by the Landau distribution of

the deposited charge convoluted with the Gaussian noise distribution and the effect of charge sharing between neighboring strips. *The median charge is measured as the charge corresponding to the threshold where 50% efficiency is obtained.* In practice, the threshold is expressed in equivalent charge and the value for the median charge is obtained directly from a fit with a skewed error function:

$$\epsilon = \epsilon_{max} f \left(x \cdot \left[1 + 0.6 \frac{e^{-\xi x} - e^{\xi x}}{e^{-\xi x} + e^{\xi x}} \right] \right)$$

where f denotes the complementary error function. The median charge μ , the width σ , the skew ξ and the maximum efficiency ϵ_{max} are free parameters and $x = (q_{thr} - \mu)/\sqrt{2\sigma}$. Each data point corresponds to the efficiency measured on a single run of 10000-15000 events.

The error on the median charge is dominated by the uncertainties in the calibration. The variation of the calibration from one chip to the next is evaluated in the beam test by pointing the beam to areas of the detector read out by different chips and measuring the median charge of each chip separately. Correcting the charge of each chip by measurements of the calibration DAC output improves the uniformity, taking into account the spread in median charges due to variations in the components of the calibration circuit. In practice, comparison between different modules is greatly facilitated by the use of the signal-to-noise ratio, the ratio of median charge and the equivalent noise charge.

A theoretical expectation for the signal height is obtained from a GEANT4 simulation of the energy deposition by the beam particles (protons, pions, or muons) in 320 μm of silicon. The number of electron-hole pairs created along the track is obtained by dividing the deposited energy by the average energy required to produce an electron hole pair, 3.63 eV. The electron contribution to the signal is expected to be small. Ignoring the electron contribution, the signal induced on the readout strip is taken to be the sum of the charges of the holes. Under this assumption the median signal is calculated and compared with the results of the measurement. Any discrepancy between the deposited and collected charge must be understood.

Charge shared between neighboring strips cannot be re-clustered in the binary readout scheme as it is predominantly below threshold. Diffusion of the charge carriers while they drift toward the readout plane can be studied using the position predicted by the telescope. Cross-talk between neighboring channels is expected to be responsible for a charge loss on the order of few percent. Finally, the charge carried to neighboring strips by δ -electrons can be quite substantial. However, GEANT4 model calculations show that even though this effect leads to a less pronounced high-energy tail in the charge distribution, the median charge is not significantly affected.

4.7.11 Detector Bias Voltage

The bias voltage of the detectors is an important operating parameter and the bias voltage dependence of the performance is studied in detail. The bias voltage dependence of the efficiency at a threshold of 1 fC is measured. For overdepleted sensors the median signal-to-noise ratio is nearly constant and charge collection efficiency should be close to 100%. As the bias voltage is decreased towards the depletion voltage (around 75 V for the SVT sensors) the signal might gradually decrease. This can be explained as a ballistic deficit of the shaper circuit, i.e. the integration window of the front-end electronics is no

longer large compared to the charge collection time of the detector, leading to charge loss.

4.7.12 Charge collection in the inter-strip region

In order to investigate the charge sharing, the median charges are calculated according to the beam particle position. The positions midway between the strips, with a width of 20 μm , are defined as the inter-strip region. The positions around the strips, with a width of 40 μm , are defined as the strip region. The ratios of the median charges in the inter-strip over the strip regions are calculated and plotted as a function of the detector bias voltage. The uncertainties associated with non-uniform damage, imperfect calibration of chips, absolute amount of charges collected, etc., are largely eliminated by taking ratios.

4.7.13 Incidence angle and magnetic field

In CLAS12 experiment the SVT modules are situated within a 5 Tesla magnetic field. Also, tracks will not generally be perpendicularly incident on the detector plane. Therefore, an important subject of study is the influence of the magnetic field and incidence angle on the performance of the modules. One of the goals of the beam test is to investigate the dependence of the most important parameters - efficiency at the operation threshold, median collected charge, and spatial resolution - on the incidence angle and field. Two orthogonal orientations can be studied. When the projection of the particle trajectory on the read-out plane is parallel to the strips, the longer path length through the silicon leads to an increase of the median charge with $1/\cos(\alpha)$. In the second orientation the projection of the particle trajectory is perpendicular to the strips. The longer path length again leads to a small increase of the signal. But, in this orientation the projection of the particle trajectory on the readout plane is perpendicular to the readout strips. For large incidence angles the projected distance becomes significant compared to the pitch and charge sharing between neighboring strips becomes important. The net effect is a decrease of the median collected charge on a single strip.

In a strong magnetic field the Lorentz force deviates the drifting carriers. Figure 30 shows how the Lorentz force is equivalent to a rotation by a small angle $\Theta_L = \mu_H B = r_H \mu B$, where μ_H the Hall mobility, the conduction mobility μ multiplied by the Hall scattering factor r_H . In p+n type sensors, the signal is predominantly due to holes and the Lorentz angle is of the order of a few degrees.

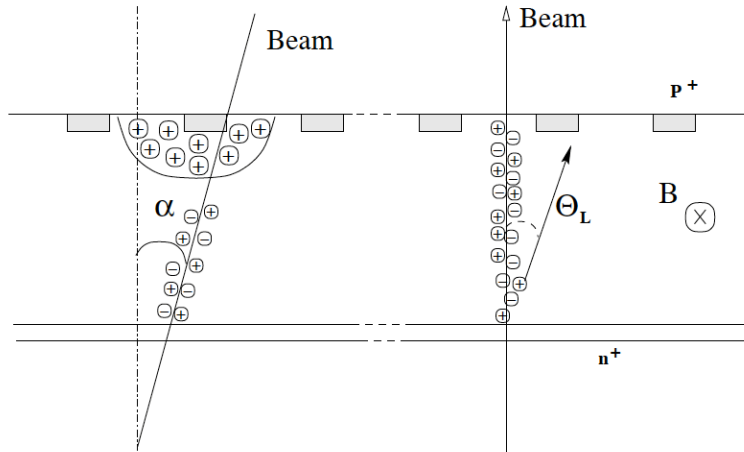


Figure 30. Representation of the effect of the incidence angle and the application of a magnetic field.
The angle α is the incidence angle of the beam particle, Θ_L is the Lorentz angle of the drifting carriers.

A sensitive measure of charge sharing is the average cluster size. The cluster size dependence on angle in a magnetic field is used to determine the Lorentz angle. Noise clusters are excluded by placing a 200 μm window around the track position predicted by the telescope. The increase of cluster size at non-perpendicular incidence reflects the increased charge sharing. The effect of the magnetic field is a shift of the distribution by the Lorentz angle. The value of the Lorentz angle is determined as the minimum of the cluster size versus angle curve. The spatial resolution depends on the number of strips in the cluster. An increase in the number of multi-strip clusters is expected to lead to a better resolution.

4.7.14 Edge measurements

It is important to verify that the detectors remain efficient at their edges, noise is comparable with average noise of the chip, and that the residuals are not significantly distorted by edge effects. To investigate the behavior of the modules near their edges, some of the runs can be taken with modules offset so that the beam passes through the corners of the detectors. The residuals as a function of the projected perpendicular position of the track from the center of the first active strip (the closest to the edge strip is passive, i.e. not connected to the preamplifier) are analyzed. Module must remain fully efficient to the center of the last read-out strip, beyond which the efficiency will drop rapidly over a distance of tens of microns since beyond this point the majority of the charge will fall in the inactive region.

4.7.15 Timing measurements

In the conventional beam test analysis described in the previous sections events from a narrow trigger phase window are selected to optimize the sampling time with respect to the charge deposition time and thus evaluate the module performance in an environment similar to the expected operation in CLAS12. An alternative approach is to explicitly reconstruct the dependence of collected charge (if any) on the charge deposition time. The pulse shape reconstruction takes advantage of the fact that test beams are normally continuous, i.e. the sampling time varies randomly over the length of a BCO clock cycle - 128 ns. The relative charge deposition time is measured as the delay between the raw trigger from the scintillators and the next rising edge of the BCO. The measured time range is extended to cover 384 ns using the hit information from the previous and next clock cycle.

Combining the efficiency versus time dependence for all runs of a threshold scan provides a 2-dimensional map of efficiency versus time and threshold. For each 1 ns time slice, the variation of efficiency with comparator threshold forms an S-curve. As in the previous analysis, the threshold is expressed as the equivalent charge injected to the front-end obtained from the response curve. The median charge for each time slice is found as the threshold where 50% efficiency is obtained (V_{T50}). The fit function is replaced by a complementary error function to ensure a robust fit of the out-of-time bins. The resulting charge versus time curve represents the median time-resolved input of the discriminator. A possibility of an extra delay in the discriminator for signals with a small

over-drive (i.e. signals that are close to the threshold) is verified.

Inefficiencies due to out-of-time hits and the occupancy load of these hits in the consecutive event (ghost hits) are studied. A too small time interval between the trigger and the edge of the BCO clock could lead to out-of-time hits that have the time-stamp of the consecutive bunch crossing. These (ghost) hits might not be assigned to the track and thus can be a source of inefficiency. Moreover, they might add to the occupancy of the consecutive event. The ghost hit occupancy depends on the signal occupancy and the probability that a track leaves a ghost hit in the subsequent clock cycle. Ghost hit probability should yield a maximum occupancy insignificant compared to the allowed noise occupancy. Some charge is shared between two strips through dispersion of charge in the silicon or cross talk due to the interstrip capacitance. Small charges due to charge sharing are likely to give a late discriminator response (time walk) and can thus appear in the clock cycle subsequent to the triggered cycle.

5 Detector control and safety system (DCS)

In order to maintain proper performance of the SVT, all critical characteristics of the system are tracked. This monitoring operation can be described by three types of operations:

1. Monitoring of all parametric characteristics of the SVT, such as voltages, currents and temperatures
2. Periodic calibration of the detectors and readout electronics
3. Monitoring of the quality of data being collected by SVT and passed to the Trigger/DAQ (Figure 31).

5.1 *Monitoring of SVT Operating Parameters*

The monitoring of the SVT detector is split on several nodes of the Detector Control and Safety System (DCS/DSS). Most monitoring can be done outside the SVT detector where the services are generated.

For monitoring in radiation environment inside the SVT enclosure the aim is to have as few complex active elements as possible but the choice of technique also has to take into account the amount of material which is introduced into the tracker. The sampling frequency of the monitoring is not foreseen to exceed 10 Hz for a full set of parameters. In the event of a power failure the monitoring will continue to run on uninterruptable power supplies. The SVT DCS will monitor the following parameters:

- the low voltage and current
- the high voltage and current
- the temperature of the modules
- the humidity inside SVT
- the radiation inside the SVT
- the status of the cooling system

The monitoring of voltages and currents is made at the power supplies. It is believed that the voltages at the module can be known to a precision better than 2.5% of nominal value even without remote sensing. Temperature monitoring is done within the high radiation environment. The humidity is monitored inside the SVT enclosure. The environment data is needed for the alignment system. The SVT is flushed with dry nitrogen. The monitoring system must sense small amounts of water vapor.

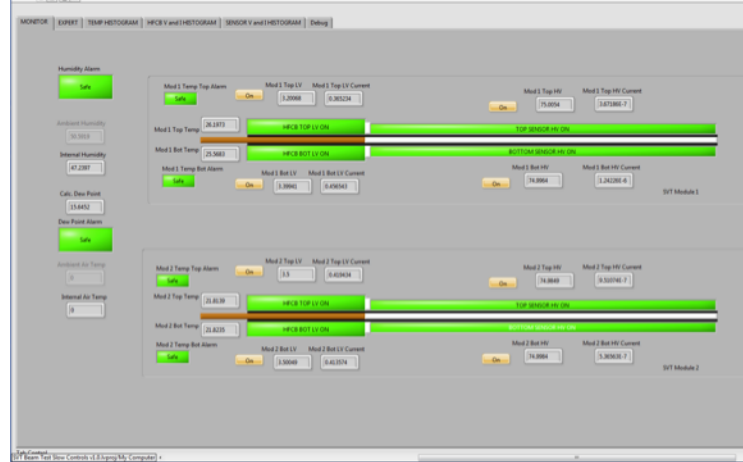


Figure 31. VXS controller GUI for boot configurations and VSCM monitoring.

5.2 Calibration of Detectors and Readout Electronics

The front-end electronics has a built-in calibration facility, which allows charge pulses to be injected into the front end of the amplification stage upon request from the SVT Control System. The quantity of charge, the timing of the charge pulse and the sub-set of channels pulsed can be controlled by commands to the front-end chips.

With the binary readout architecture, the principal calibration procedure is to either vary the amplitude of the injected charge with fixed threshold or to vary the threshold with fixed amounts of injected charge. For each calibration pulse, the resulting status of the comparator (either hit or no-hit) is recorded. Result of one of these scans plotting detection efficiency as a function of threshold for a fixed input charge. The “S” curve response is typical showing 100% efficiency at low threshold and falling away to 0% efficiency at very high threshold. The point where this response crosses 50% locates the mean value of the injected charge distribution. The width of the transition region (from 100% to 0%) measures the width of the distribution of charge measured at the comparator. For the case of calibration pulses of fixed amplitude, this distribution is, in fact, the composite noise of the readout system. A quick scan of each channel provides an easy measure of the overall gain of the analogue section (i.e. the 50% point) and the noise. Since the charge is injected at the very front of the readout stage and propagated through the entire chain, these calibration procedures provide an excellent diagnostic for the entire readout system.

The full calibration procedure will scan the threshold for a series of calibration pulses on each channel and collect the data. A quick fit of an error function to the “S” curve for each channel will produce the mean pulse amplitude and the standard deviation of the

noise for that channel. These two values will then be stored in the historical trend charts for each channel and compared against allowed statistical limits.

The operation of this calibration procedure for the whole of SVT will simultaneously pulse several channels on each module and read out the “hit” data. The repetition rate is approximately 200 kHz so that 1,000 points can be accumulated for an “S” curve in a fraction of a second. Since each module has a completely independent readout chain, the entire SVT can be thus calibrated within minutes. The 200 kHz rate can be handled easily by the available bandwidth and the 1,000 points will provide sufficient accuracy in determining the mean and standard deviation of the distributions for historical monitoring.

This calibration procedure is intended to spot slow drifts in the SVT performance. Dramatic changes in operation resulting from, for example, a dead channel, are most likely spotted by monitors of the Data Quality discussed in Section 6. Therefore, this calibration procedure needs only to be run once every few days and this can be accommodated during run changes or other non-data taking periods so as not to introduce dead time into the experiment.

SVT DAQ will have the capability to supply samples of event data to the DCS for the monitoring of data quality. The occupancy of each channel or strip is accumulated and filtered. Sampling of the triggered data is random at a rate determined by the processing power of the DAQ. Given the expected occupancy of each channel, statistics for these occupancy measurements accumulate very quickly and deviations from the norm are immediately reported. Occupancies averaged over periods of approximately one hour are recorded in a short-term database with longer averages held in permanent storage.

It is possible to collect statistics on other aspects of the event data as specified by filters given to the DAQ. This may be used to look for more subtle correlations in the data. The possibility of using fitted tracks to measure real channel efficiencies using a 3 out of 4 point requirement is being investigated. The ability to do this is limited by the available processing power for these on-line monitors.

6 Data Quality Monitoring

Aiming for a homogeneous monitoring environment across various applications related to the data taking with SVT, the Data Quality Monitoring (DQM) system is arranged. The primary goal is to ensure the quality of commissioning, calibration, and physics data collected in general data acquisition. The main requirement for DQM is maximum flexibility so it can be used at various stages of detector integration and commissioning interactively, e.g. update of histogram code on request. In addition, DQM has to have the least interference with data taking, triggering and data storage. Hence possible problems in DQM can be isolated and CPU-intensive tasks will not slow down the general data taking in CLAS12 DAQ.

6.1 DQM architecture

Following the requirements above, the DQM framework is designed in three main layers. The basic DQM components, monitoring elements (ME’s: histograms, floats, integers, strings), are produced in source s, which retrieve the event data information

from several storage managers, SM's. DQM source fills information from different levels of reconstruction: digi (#digi per detector, amplitude, ...), cluster (cluster charge, position, width, ...), global track parameters (momentum, Θ , ϕ , ...), on/off track clusters (cluster properties), and residuals. Source has access to conditions DB for cabling, calibration data, magnetic field, geometry etc. Event source can be file or SM. Sources are connected to a collector in a many-to-one structure. The collectors are responsible for the redistribution and periodic update of monitoring elements on one hand and on the other hand they act like servers for the final users, the clients. The client is blind to the source; the source remains stable and will not be slowed down. Also, the quick transfer of monitoring information from sources to collectors is facilitated. A client needs to subscribe to the collector, requesting for a subset of monitoring elements, which are finally shown to the end user in a histogram format. DQM client performs analysis of the ME, produces summary MEs from module level ones, creates the Tracker Map, and defines global and region states from the module level alarms. Quality tester monitors data quality and assigns "ok", "warning", and "failed" flags. The Graphical User Interface, GUI, serves the centralized visualization of the DQM histograms.

Although DQM works with event data, it does not give access to individual events since it has a statistical nature. What is seen on histograms is collected over a period of time so punctual problems are not spotted.

6.2 DQM Operation

Data Quality Monitoring is performed online and offline. While the online DQM is carried out to support the prompt reaction about the detector status based on a subset of data, the offline monitoring is done with some latency and has two main steps, which finally end up in data certification for physics analyses. In the first step a subset of data, the express stream, is reconstructed and monitored within about an hour. The goodness of run is examined in terms of the reconstruction software, calibration and alignment constants. After about 48 hours the full dataset is reconstructed with better constants obtained in the previous step. Another offline monitoring sequence is performed when the data is reprocessed and re-reconstructed with new software releases.

To certify the goodness of data in both online and offline monitoring, first some test algorithms are run automatically, checking different parts of the detector and reporting possible problems in the DAQ, etc. Then a shifter is in charge to investigate the goodness of data by looking at the most important distributions and a quality indicator is assigned to each subsystem. The manual certification is registered in the Run Registry that is the central workflow tool for DQM, tracking certifications and quality knowledge. It has an interface with SVT Data Bookkeeping Service in which one can find the results of the automatic certification as well. Once the final certifications are confirmed for different runs and the runs are "signed-off", a list of GOOD runs is prepared. Finally for physics analyses, the certification can even be more specific, resulting in qualified luminosity sections

within runs. This information is saved in files with the Java Script Object Notation (or JSON) format and can be used while running the analysis on the relevant dataset.

6.3 *History plotting tool for DQM*

The History DQM takes care of the extraction and visualization of the summary information obtained from the run-based DQM histograms. History DQM (HDQM) consists of two steps:

1. Extraction and storage of the relevant information in the condition database: For each histogram corresponding to a selected quantity the derived summary values are extracted and stored in the CLAS12 database. The list of selected quantities is flexible and adapted to every DQM task.
2. Creation and visualization of the trend charts (**Figure 32**): Two complementary approaches allow accessing the summary information.

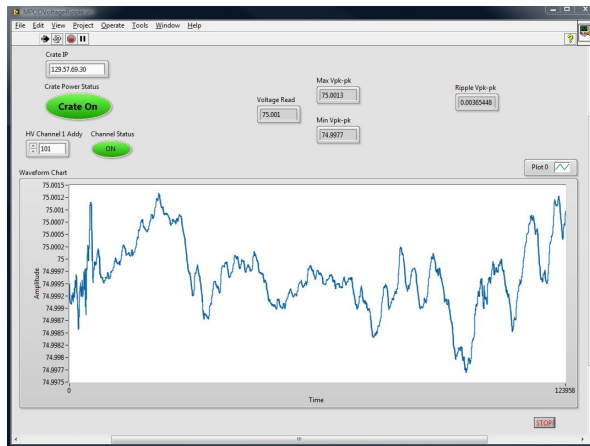


Figure 32. Historic DQM GIU for monitoring HV power supply.

- (a) A root based approach: intended for experts to be able to perform detailed analyses.
- (b) A web approach: intended for prompt feedback.

Several default quantities are available, such as Gaussian fit mean and sigma or Landau fit peak and width. It is also possible to provide user-defined fit functions.

The interaction of the HDQM with the CLAS12 allows the CLAS12 offline software to access the calibration data. The database schema accepts and stores a configurable number of summary information for a configurable and dynamic set of detector elements. This approach allows storing data at different granularity levels and guarantees the backward compatibility in case of an extension of the list of monitored quantities.

The Root based inspection of the HDQM database for the trend plot creation is designed for an expert usage. A Root macro interface allows querying the database and extracting trends and correlations in a tree-like approach. The HDQM contributes to the characterization of the detector over time. The main quantities related to the SVT (number of reconstructed tracks and hits, signal over noise of the reconstructed signal, etc.) are automatically extracted from the corresponding histograms and stored in the HDQM database. The analyses are performed to tag the (good/bad) status of the

registered runs. The Root based interface is exploited to correlate the stored information in the database and to identify the properties of the runs deviating from the reference.

6.4 Interactive SVG Maps and Web Services for SVT monitoring

SVG is already being used in HEP (and outside HEP) visualization tools as a standard way to export 2D graphics. For this use it can replace the postscript format since it has the same capability to represent vector graphics (shapes, text and embedded images). If you compress the text file, it is also more compact. SVG images can be zoomed and panned exactly like postscript images. By adding JavaScript code other interactive features can be added. In our case the most important are:

- the possibility to pick a part of the image getting information about the detector part represented in the detail.
- the possibility to connect the image to web services that will provide new data refreshing the image.
- Since SVG is an XML instance, it should be supported by all browsers which are XML-compliant clients.
- Monitoring the SVT requires access to the following data sources:
 - construction database (this is a single database containing for example list of dead channels in the module)
 - DDD (Detector Description Database) - Description of detector geometry.
 - conditions database (working conditions for each module: voltages, temperatures, etc.)
 - last events read from detector
 - histograms database

Since each data source has a different API, a single XML format for tracker data is defined and instead of accessing the data directly, web services that act as gateways to data sources are used. The data is transformed in this xml format and sent back to the SVG image when the user requires new data to display. The data about the geometry are only accessed once, at the beginning of an interactive session, and produce the sending of the SVG image itself. In some cases, when the data to be sent is too much, it can be transferred directly in the SVG format (instead of XML) and replace completely the previous image instead of only refreshing it.

In the past the main visualization tool for monitoring was a histogram presenter that would show a set of histograms and tables updated regularly. The SVT has tens of thousands channels organized in modules each one being a complete detector: its monitoring requires many hundreds of histograms to be computed every few minutes. A histogram presenter is not enough: people in charge for monitoring need a representation that would show all modules at once in a single computer screen with single modules information coded in some way. This is the representation implemented in the SVG image. This "tracker map" is obtained in the following way: since the single module is flat, we imagine to disassemble the whole tracker and to assemble it again on a flat surface putting the single modules in positions which are connected to their spatial position. Data from each one of the data sources described in the previous paragraph can be represented on this map. For example the single module can show coded with a color:

- number of dead channels from construction database
- total number of RecHits hitting the module in the last 100 events readout

- result of a comparison between the last histogram and a control histogram

Holes or hot spots in the map can pinpoint detector problems. In this case the interactive nature of the map is essential. In this use for Web monitoring, the map has the additional advantage of minimizing data transfer (this map can be used also locally in the control room).

Tracker map should be implemented in geometric and readout views, control and PS views.

A monitoring program working in the control room can save every few seconds on a server Web an SVG image with the integrated signal map for the last events. An expert can with a normal browser access it and check that everything is ok with all modules of the tracker.

Web Based Monitoring (WBM) tools are used by:

- Expert and shifters to check out and commission the SVT:
 - Verify that information is correct in the DB
 - Diagnose problems (use DCS, configuration, and commissioning analysis information)
 - Software testing in production context
 - Test the scalability of the system (software and hardware)
- Developers:
 - Analyze the problems
 - Fix discovered bugs
 - Implement new functionality

WBM solutions work at the level of information and then are contributing to the durability of understanding the database schemes:

- Until the SVT is commissioned (unstable state):
 - DB schemes will evolve
 - Internet tools are used to test/debug/diagnose the system
- After the SVT is commissioned (production):
 - Recurrent queries are transferred to CLAS12 WBM (unknown at this time)
 - There is a possibility to write queries to publish information

Detailed analysis on commissioning runs can be done on:

- The histograms produced by the commissioning analysis and saved in root files
 - Specialized GUI to view the histograms
 - An offline web interface (needs development)
- Raw data files, re-running commissioning
 - Only for development/debug/deep study on specific analysis

WBM used to visualize and monitor results of commissioning analysis:

- For a given run

Trend plots as a function of time

7 Module services

Module services provide power, cooling, and communication to all the SVT modules. The services connected to the SVT include: power supply cables, data and control cables, cooling pipes, and cables for monitoring humidity and temperature. Once all the services are attached, the cooling circuits are tested for blockages, and the modules are powered, their electrical circuits are read out, checked, and repaired as appropriate.

7.1 Power supplies

The power supply system consists of low voltage and high voltage supplies. The low voltage supply powers the analog and digital portions of the readout chips. The high voltage supply provides up to 500 V for biasing the sensors and monitors the leakage current over a wide range. Full depletion voltage of the sensors is from 65 to 80 V. The ISEG high voltage power supply module residing in the MPOD mainframe (Figure 33) is capable of providing current up to 10 mA per channel with 10 mV steps and ripple less than 5 mV peak to peak. Due to the losses in cables, the actual voltage, which appears at the module end of the cable, is measured and source adjusted appropriately. Each side of the module receives low voltage, 2.5 V for both analog and digital parts of the FSSR2 chip and high voltage for the sensors. The low voltage also powers analog output CMOS IC temperature sensors, one per side. An independent floating circuit supplies each voltage to each module. This enables control of grounding and shielding; all voltages are grounded to the common spot and shields of the cables are grounded at the power supply.

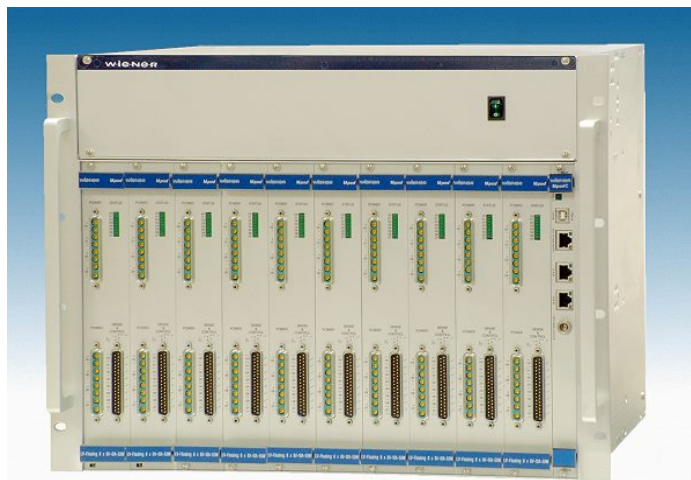


Figure 33. Wiener MPOD mainframe with LV power supply modules.

7.2 Cables

Checkout of the cable routing schemes of the signal readout with high and low voltages applied to the detectors and reading out electronic noise and currents on HV and LV lines is carried out with calibration signals injected channel-by-channel into the front-end electronics. This procedure will identify false signal cablings and faulty signal and power connections.

7.3 Cooling

The SVT requires a cooling system to keep the silicon sensors at a low temperature and to remove the heat produced in the readout electronics. Upper limits on the heat loads of the different heat sources in the SVT are calculated. Each module produces about 2 W of heat from the readout chips and up to 1 W due to the leakage current in the silicon sensors. This cannot be dissipated passively from the small SVT volume so active cooling is necessary. The modules are cooled by copper heat sinks attached to the cold plate (Figure 34) that has circulating liquid coolant.

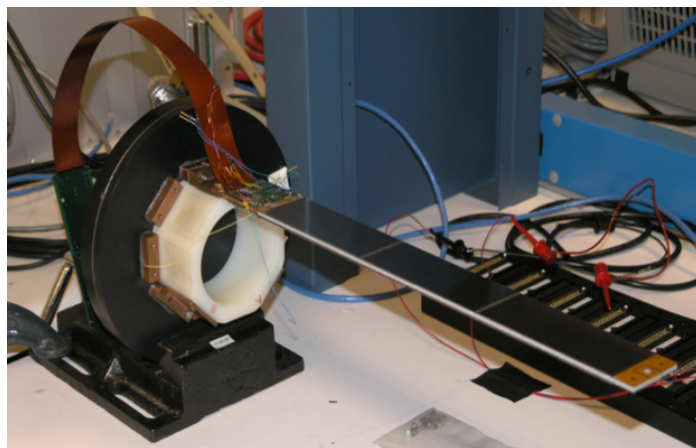


Figure 34. SVT module mounted on the cold plate for temperature measurements.

8 Tracker integration and commissioning in Hall B

8.1 Transportation requirements

Because of the delicacy of the silicon modules, it is required that the SVT be transported to Hall B in an air-sprung, temperature-controlled, humidity-controlled thermal screen mounted on a truck. The acceleration experienced by the transport box is required to be less than 3 g (where g is the acceleration due to gravity) to avoid damage to the silicon modules and shaking loose connectors. The tilt is required to be less than 10°. The temperature is required to be $20 \pm 3^\circ\text{C}$ to avoid thermal stresses and the humidity kept at around 40% and certainly less than 70% to avoid condensation forming on the modules.

8.2 Tracker integration tests

The testing during tracker integration in Hall B is focused on checking the integrity of the service connections, performance of the cooling, and then verifying that the additional components did not cause deterioration in the SVT electrical performance. This latter part of the testing is crucial in demonstrating that whole SVT system design is robust with respect to inter-module pick-up and external interferences. No significant differences should be seen compared to the results from the testing of the SVT in the assembly clean room.

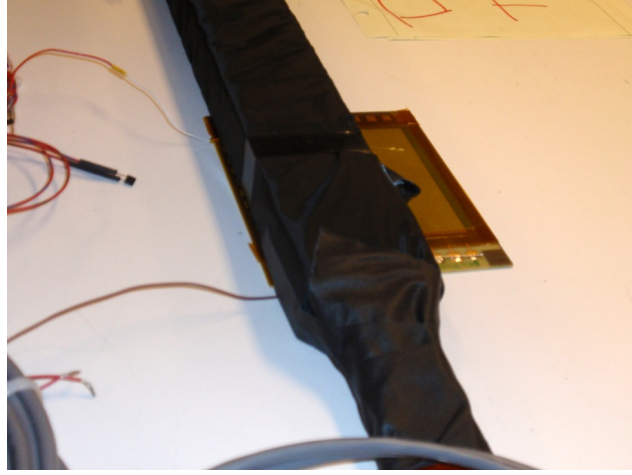


Figure 35. Measuring performance of the SVT modules in presence of the sparking Micromegas detector.

Before transportation to Hall B, the SVT is integrated with Micromegas. Further tests, including combined SVT/Micromegas cosmic ray studies, will then be performed in Hall B during detector integration and commissioning. These are the first large-scale tests of the SVT DAQ in physics mode. Several millions of physics-mode events are recorded in the synchronous operation of all SVT modules during the commissioning. In the noise tests, the occupancies obtained should not be significantly different from those found for tests made on the SVT before integration (Figure 35). No significant change in noise occupancy should be observed when running concurrently with Micromegas, when running at different trigger rates, or for synchronous versus asynchronous triggering. The data and control cable connections are monitored by the DAQ and the remainder are controlled and monitored by the DCS.

8.3 Mechanical stability and alignment

Mechanical stability and alignment are very important in a precision tracker. Figure 36 shows the model for simulating deflection of the SVT barrel. Precise determination of the position of all silicon modules is a challenging task and one of the critical aspects for achieving the design track parameter resolutions. Optical surveys are taken during module construction and integration provide initial alignment parameters for the SVT modules. Coordinate Measuring Machine (CMM) data and photogrammetry is used for the optical survey of the tracker components. While the former are used for measurements of the active elements, the latter are used for the alignment of larger structures. Both module-level and high-level structure information is stored in the construction database and used in the analysis.

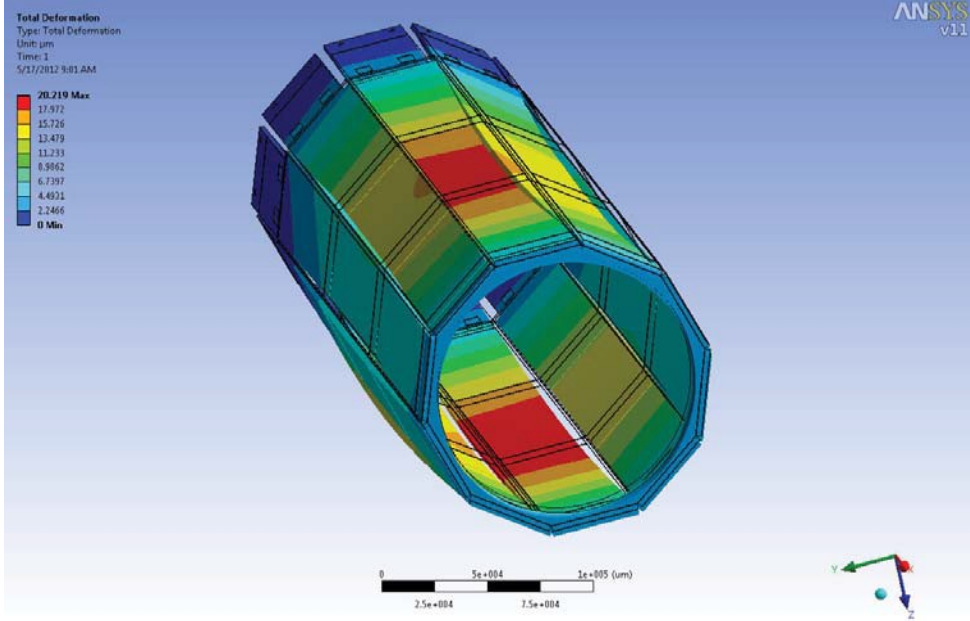


Figure 36. Deflection model of the SVT barrel.

The alignment stability of the SVT is constantly monitored using dedicated alignment calibration runs with and without magnetic field. Movements within the detector are at the sub-micron level during stable runs. Environmental changes in the detector (for example changes in temperature due to cooling stops and starts or changes in the magnetic field) result in shifts on the order of several microns. The absolute alignment is determined using tracks; track-to-hit residuals are minimized with respect to various alignment constants. Design specifications are expected to be reached when alignment is improved with higher statistics. Higher statistics will also allow time-dependent alignments. Dedicated alignment data streams have to be implemented. Alignment corrections are performed on a run-by-run basis starting from a common set of alignment constants. Large movements of the detector are measured after hardware incidents. The final alignment is possible with SVT commissioning with beam and magnet-on condition. This work is preceded with alignment of the SVT sectors using cosmic muons during stand-alone commissioning of the SVT-Micromegas without magnetic field. A dedicated cosmic track finding algorithm is used at this stage to reconstruct the cosmic muon trajectories. The result is a set of track parameters. Five track parameters describe the helical trajectory of a track at the point closest to the nominal interaction point: distance of closest approach in the transverse d_{xy} and longitudinal d_z directions, track azimuthal angle ϕ , track polar angle θ , and transverse momentum p_T . The track reconstruction uses the Alignment Position Errors (APE), the estimated uncertainty on the module position in the three global coordinates, which are added in quadrature to the hit errors during the pattern recognition and track fitting procedure. This allows efficient track reconstruction in the presence of misalignment and a correct pull distribution of track parameters. The APE values for the initial track reconstruction before alignment analysis are set to large values as they have to account for possible large displacements of the SVT vs. Micromegas while still guaranteeing an efficient track-hit association. The momentum and angular spectra of cosmic muons reconstructed in the SVT tracker volume are analyzed. Two complementary statistical alignment

algorithms, a global and a local iterative method, are applied to the data, taking into account survey data as constraints. The alignment of the SVT-Micromegas tracker is performed in subsequent steps, varying the number of degrees of freedom. The first level only corrects for sub-detectors global misalignments. The second is used to align sub-detector components and the third aligns individual mechanical units (SVT modules, Micromegas tiles). Using cosmic ray data, it is possible to complete the second alignment step and part of the third one with final alignment using beam data. Alignment algorithms are validated at this stage. Results from the alignment studies are compared extensively with detailed Monte Carlo simulations of the detector.

The track parameter resolutions can be validated with independent reconstruction of the upper and the lower portions of cosmic ray tracks and comparison of track parameters at the point of closest approach to the nominal beamline. Both the upper and lower track segments are required to have hits in all layers. The track segments are reconstructed independently and improvement due to tracker alignment is validated. The results are compared to a MC simulation with ideal detector geometry. Given the reasonable level of alignment achieved, track parameter resolutions should be consistent with the MC expectations.

8.4 Commissioning the SVT control and readout systems

To bring the SVT detector into an operational state suitable for data taking, several commissioning procedures are required to check out, configure, calibrate, and synchronize the various hardware components of the control and readout systems. The majority of the commissioning procedures are performed with the SVT operating independently of the rest of the CLAS12 experiment. Only the procedures that concern synchronization to an external trigger require reconstructed particle trajectories from cosmic ray muons or beam data. The commissioning of the SVT aims to maximize the signal identification efficiency for in-time particles and minimize pileup due to out-of-time particles. The ultimate objective is to maximize the tracking efficiency while minimizing the number of tracks caused by out-of-time signals from adjacent bunch crossings.

8.4.1 The control and readout systems

The major components of the SVT readout system are: xx front-end detector modules that host xx FSSR2 readout chips, xx digital signal readout cables, and xx VSCM readout boards. The SVT control system is also driven by the VSCM boards, which distribute the clocks and control signals to the front-end detector modules.

The FSSR2 has a data push type of readout architecture. Data is output serially from the FSSR2 using Low Voltage Differential Signals (LVDS). One feature of the data output interface is the ability to program the number of serial output lines to be used depending on the expected hit activity in a given chip. A chip with low activity can use just one output serial pair while a chip in a very active area may have as many as six output pairs transmitting data from the chip. This means that no buffering of the output data is required on the chip. The data output interface formats the information to be transmitted and adjusts the internal clocking frequencies so that all hit data in a single Bunch Crossing Oscillator (BCO) is normally read out in about one BCO time interval. The

BCO clock is run at a period of 128 ns. The FSSR2 readout clock is designed to be 70 MHz and not tied to the BCO clock. Information is read out on both edges of the readout clock for a maximum data transmission rate of 840 Mb/sec.

Status/sync information and hit information are read out at different times depending on the hit activity in the chip. A readout word is comprised of 24 bits. The status/sync word has 10 bits of status, 13 bits for synchronization, and 1 bit for a word mark. The data word has 8 bits for the BCO number associated with the hit, 5 bits for the number of the logic set handling the hit, 4 bits for the number of the hit channel within a set (there are 16 sets with 8 channels in each set), 3 bits for ADC data, and 1 bit for a word mark (3 bits are unused). Data sent from the chip is not time ordered. The BCO number is used off-line to reconstruct beam interactions. Since point-to-point communication is used, no chip ID information is needed in the data output.

8.4.2 Checkout of the detector components and cabling

The checkout procedures are used to identify: responsive and functional devices in the control and readout systems; the cabling of the readout electronics chain, from the front-end detector modules to the off-detector VSCM boards; the cabling of the low voltage (LV) and high voltage (HV) buses of the power supply system; and the mapping of the detector modules to their geometrical position within the SVT structure. The cabling of the LV power supply system is established by sequentially powering groups of detector modules and identifying responsive devices via the control system. Similarly, the HV cabling is determined by applying HV to an individual channel and identifying detector modules responding with a decreased noise, due to reduced strip capacitance. Problems in the readout chain should be fixed, mostly by replacing the faulty component (e.g. electronics board, patch panel, cable, connector). The fraction of operational modules should be kept close to 100%, once problems identified during checkout are fully investigated.

8.4.3 SVT slow controls

The slow controls procedures to adjust the critical parameters of the detector are checked out once the full system has been installed in Hall B as part of the general CLAS12 commissioning plan. It will include checkout of all systems controlled by EPICS.

8.4.4 Relative synchronization of the front-end

Relative synchronization involves adjusting the phase of the BCO clock delivered to the front-end with the main accelerator clock. This synchronization is important because the BCO clock number is used to associate the SVT hits with the CLAS12 trigger.

8.4.5 Calibration of the readout system gain

One of the largest contributions to gain variation in the readout system is the chip-to-chip variation of gain. Changes in the chip LV or environmental temperature can also affect the gain of the readout channel. The response of all detector channels can be further equalized during offline reconstruction by correcting the signal magnitude by the normalization factor. This procedure is verified in further studies due to low granularity (3 bit) of FSSR2 Flash ADCs.

8.4.6 Cosmic ray calibration

This commissioning procedure includes synchronization of all modules in the SVT with the Level-1 trigger of CLAS12. This is done using a dedicated trigger provided by the Central Time-Of-Flight (CTOF) detector, based on a coincidence between centrally located top and bottom chambers. The procedure requires track reconstruction and the analysis performed offline. Absolute synchronization accounts for the delays introduced by the hardware configuration and the effects due to the time-of-flight of particles.

After complete assembly and installation of the central detector system, cosmic ray triggers by the additional start counter in the CTOF barrel are used to measure the efficiency of the SVT response and the track reconstruction, first with straight tracks without magnetic field, and then with the solenoid magnet ramped up to 1/2 and full fields, to test the accuracy of track reconstruction in the barrel part. For this, the track is reconstructed in the eight SVT layers in the upper hemisphere, and checked against the track parameters reconstructed in the eight SVT layers of the lower hemisphere. Agreement within multiple scattering effects is expected.

8.5 Performance of the local reconstruction

This section addresses the reconstruction at the level of the single detector module. The cosmic ray muon rate is small, and events with more than one track are rare. So with zero-suppression, only a tiny fraction of the SVT channels are read out in any one event. These channels, which pass zero-suppression and therefore have non-zero ADC counts, are known as digi. Despite the zero-suppression, digis may still only consist of noise. Clusters are formed from digis by means of a dedicated threshold algorithm (TBD). Clusters are seeded by digis that have a charge that is at least x times greater than the corresponding channel noise. For each seed, neighboring strips are added if the strip charge is more than x the strip noise. A cluster is kept if its total charge is more than y times the cluster noise, defined as $\sigma_{cluster} = \sqrt{\sigma_i}$, where σ_i is the noise from strip i , and the sum runs over all strips in the cluster. The properties of both digis and clusters are studied, and the performance of the SVT is assessed.

8.5.1 Occupancy

The average number of digis per event and the occupancy are extracted from the data. The strip occupancy is computed after removing the masked channels. The average occupancy in the SVT is compared with the number expected from simulation and from the properties of the zero-suppression algorithm. The digi occupancy is dominated by noise, but the cluster algorithm should be able to reconstruct less than ten hits per event when there is no track within the SVT acceptance.

8.5.2 Signal-to-noise ratio

The signal-to-noise ratio is a benchmark for the performance of the SVT. It is particularly useful for studying the stability over time. In the signal-to-noise ratio, the cluster noise is divided by $\sqrt{N_{strips}}$, so that the resulting noise value is approximately equal to the strip noise, independent of the size of the cluster.

8.5.3 Gain calibration

The charge released in the silicon sensors by the passage of a charged particle is processed by the readout electronics chain described in section 8.4.1. The ratio of ADC counts output after digitization to the originally released charge corresponds to the gain of the electronics chain. It is important that nonuniformities in gain are accounted for and that the conversion factor between deposited energy and ADC counts (with 3-bit limitation imposed by the FSSR2 chip) is measured correctly.

A dedicated calibration loop is being implemented which contains procedures for calibration runs, storing of the calibration constants in the database, automated analysis, and validation procedure before any changes in the calibration data are approved.

8.5.4 Lorentz angle measurement

In the silicon sensors, the electric field is perpendicular to the strips. For normal incidence particles, typically only one strip is hit and the cluster size increases with the angle of incidence. In the presence of a magnetic field, however, the drift direction is tilted by the Lorentz angle. The Lorentz angle is measured for each individual module by making a profile plot of cluster size versus the tangent of the incidence angle. The Lorentz angle correction applied to clusters during track reconstruction is relatively small—of the order of 10 μm —but if it is larger than the overall alignment precision the alignment procedure can provide a useful method of crosschecking the Lorentz angle measurements. In particular, it is useful to compare the residual distributions from data with and without the magnetic field applied.

8.5.5 Hit efficiency

The hit efficiency is the probability to find a cluster in a given silicon sensor that has been traversed by a charged particle. To calculate the hit efficiency, track seeding, finding, and, reconstruction must be performed. This is done using the Track Finder for cosmic ray muons events, excluding the clusters in the layer of the SVT for which the hit efficiency is to be determined. The efficiency for a given module in this layer is then calculated by finding tracks that pass through that module and determining if a cluster is present. Typical inefficiencies measured in this way are on the order of a fraction of a percent. The analysis is limited to events that contain only one track, which is required to have a minimum of x hits and no more than y missing hits. To ensure that the muon has actually passed through the module under study, the location of the extrapolation of the track trajectory on the module surface is required to be no closer to the sensor edge than five times the position uncertainty of the extrapolated point.

These measurements should be compatible with the expected overall percentage of excluded channels. If the channels that are excluded because of known problems are ignored in the efficiency calculation, the resulting efficiency should be greater than 99% for most layers.

9 Online software

The SVT online software is a collection of packages designed to form a common foundation for all CLAS12 software running online. This provides an infrastructure,

which is used to create a distributed system where all the sub-detectors remain under central control while changes may still be made at a local level.

The user interface enables the user to start up and shut down the system using a series of run levels. This provides a uniform user interface for all sub-detectors, while allowing individual parts of the system to be temporarily removed.

10 SVT DAQ system and commissioning software

The SVT data acquisition software is based on the CLAS12 online framework, which provides a core set of services and tools.

The SVT data acquisition (DAQ) software implements the procedures required by the various commissioning tasks. The implementation comprises dedicated DAQ loops that determine optimized configuration parameters and calibration constants from reconstructed calibration pulses, timing delay curves, dynamic range (response) curves and other features of the FSSR2 data stream. These optimized configurations and calibrations are then uploaded to the SVT online configuration database and provide the basis for subsequent commissioning tasks or physics run. Each DAQ loop is defined by a run comprising several consecutive spills of events, separated by periods when the trigger is inhibited and the configuration of a device is changed via the control system. The configuration of several devices of the same type is usually tuned in parallel.

The DAQ loops require communication between various “Supervisor” processes that control the trigger system, hardware configuration, readout, event building and data analysis. The SVT DAQ framework provides this functionality and allows automating the data acquisition loops, so reducing the need for repetitive run control sequences and complex book keeping. Consequently, this accelerates detector commissioning and start-up.

The complex control and readout systems require sophisticated procedures to bring the detector into an operational state that is suitable for physics. These commissioning procedures comprise several independent tasks that fall into one of the following categories: optimization of the hardware configurations; synchronization of the entire system, both internally and to CLAS12 trigger; determination of low-level calibration constants that are used by the hardware and, in some cases, the CLAS12 reconstruction software. These procedures are used to validate the operational functionality and performance of the detector during the Start-Up phase of the experiment and will also be performed (with varying frequencies) between fills to guarantee optimum detector performance during the subsequent period of data taking.

Several procedures have already been defined that concern either individual electronic components of the readout system or system-wide aspects. The most pertinent tasks are identified below:

- **Detector partitioning:** automated hardware scans that detect all front-end devices
- **Front-End FSSR2 Chip:** tuning of various parameters and settings.
- **Readout system:** gain matching across the entire system, optimization of dynamic range usage, determination of calibration constants for the zero suppression algorithms (and reconstruction software).
- **Timing:** “internal” synchronization of the front-end, which effectively accounts

for signal propagation delays in the control system; “global” synchronization to the trigger

11 Data samples and Monte Carlo simulations

The performance of the tracker is analyzed using the data collected during module production, SVT integration, and commissioning. The event reconstruction and selection, data quality monitoring, and data analysis are performed within the CLAS12 software framework. The data quality is monitored during both the online and offline reconstruction. The data are categorized and the results of this categorization procedure propagated to the CLAS12 Dataset Bookkeeping System. Only runs, for which the quality was certified as good, i.e., no problems were known to affect the Trigger and Tracker performance, are used for the analysis. The data samples used for the SVT commissioning are filtered to include only events that contain at least one reconstructed SVT track or that have a track reconstructed in other detectors whose trajectory points back into the SVT volume.

Cosmic ray calibration analyses use a simulated sample of cosmic ray muons to derive correction factors and compare results. Channels known to be excluded from the readout are masked in the simulation.

An automated software validation procedure has to be implemented, which would reveal any possible side effects from the proposed changes in the simulation and data processing code before they are approved.

12 Track reconstruction

Track reconstruction aims to accurately reconstruct the trajectories of charged particles. Reconstruction of the common intersection point of a set of particle trajectories helps to identify the decay point, or vertex, of unstable particles.

The SVT modules are constructed from two triplets of microstrip sensors glued back-to-back with a variable stereo-angle providing a two dimensional measurement. The sensors are rectangular with strips nearly parallel to the beam axis and variable pitch due to the fan geometry. The azimuthal angle ϕ - essential to the transverse momentum determination - is measured with high precision. The modules also provide a measurement with limited resolution in the coordinate z along the beam axis. The third coordinate is given by the sensor position.

A common software framework is needed for the large set of software applications used for the reconstruction and simulation of events in the CLAS12 detector. The software is designed to reconstruct data taken by the CLAS12 detector and also to produce simulated events.

The steps to simulate and reconstruct events:

- **Event generation:** The physics processes are described in event generators, such as PYTHIA, which simulate the particles and their momentum four-vectors.
- **Detector simulation:** The second step is to simulate the interactions of the generated particles with the material in the detector. This task is performed using the GEANT program and a detailed description of the CLAS12 geometry and the

material distribution in the SVT detector. The GEANT algorithms transport the particles through the magnetic field and simulate material interactions, such as multiple scattering, energy loss, and photon conversions and the decay of unstable particles.

- **Detector response:** At the next stage, the response of the detector, including electronics, is simulated. This step is also called digitization. If a particle hits a detection volume (like a silicon sensor), a ‘hit’ is registered in the simulated detector response. The digitization consists of simulating the response of the detector to the energy deposits in these hits. Both the response of the detector and of the electronics are simulated. The output format of the detector response simulation is equivalent to the real data after the byte stream conversion and mapping take place.
- **Reconstruction:** Starting from the detector response data, which can be real or simulated, various algorithms are used to reconstruct the event. This includes algorithms that perform pattern recognition, track fitting, vertex determination, energy measurement, and particle identification. On simulated data, the reconstructed objects can be matched and compared to the simulated input to validate the performance of the CLAS12 reconstruction software.

All the calibration data required by the event reconstruction are stored in the SVT conditions database where it can be accessed by the different software applications. Calibration constants are used to convert various raw detector data in position or energy measurements.

12.1 Track reconstruction algorithms

A large number of charged particles are produced in the electron-nucleon collision of the CLAS12, resulting in a large number of hits in the SVT detector. The track reconstruction software has to distinguish the hits from the different charged particles and determine a trajectory that best matches the measurements. The framework takes care of the order of running the requested algorithms, and it offers various common services used by the different algorithms, such as access to information about the detector geometry, magnetic field, and calibration constants.

12.2 Track reconstruction efficiency

The track reconstruction efficiency for the dedicated cosmic finder algorithm is measured using two different methods. First, the efficiencies are measured by searching for a reconstructed track and matching it to a muon triggered by the CTOF. In the second method, the efficiency is measured using data just from the tracker, by reconstructing tracks independently in the upper and lower hemispheres of the tracker.

12.2.1 Track reconstruction efficiency using muons triggered by the CTOF

In the first method, the track reconstruction efficiency is measured with respect to muons using information from the CTOF and required to point within the geometrical acceptance of the tracker. This ensures that the muons have been identified independently

of the tracker. The muons are first identified combining the data from the scintillators located in the top and bottom hemispheres of the CTOF.

The cuts are imposed on the CTOF muons to ensure that the tracks cross most of the layers of the tracker and cross most modules perpendicularly. The efficiency is then measured by searching for a corresponding track reconstructed in the tracker. The efficiencies measured in the data are compared with predictions from the Monte Carlo simulation.

12.2.2 Track reconstruction efficiency using tracker data only

In the second method, the efficiency is measured using data from the tracker; no CTOF information is included. As cosmic ray muons pass through the tracker from top to bottom, the tracker is divided into two hemispheres along the $y = 0$ horizontal plane for this study. The tracks are reconstructed independently in the two hemispheres. Tracks reconstructed in the upper hemisphere are referred to as top tracks and those reconstructed in the lower hemisphere as bottom tracks. Tracks in one hemisphere are used as references to measure the efficiency in the other hemisphere. To reconstruct the two track legs independently, only seeds with hits in the top or bottom hemisphere are selected, and the hits in the other hemisphere are removed from the track before the final track fit. To ensure that a matching track can be reconstructed, the extrapolation of the reference track into the other hemisphere is required to cross at least four layers. The efficiencies measured in the Monte Carlo simulation should agree very well with those measured in the data once the known detector inefficiencies are accounted for in the simulation. This would indicate that the tracker and the reconstruction algorithms are well understood.

12.3 Track parameter resolution

The track reconstruction can be further validated using the cosmic ray data sample by splitting the tracks into two separate parts. A measure of the resolution of the track parameters can be determined by comparing the two legs of the split tracks. To perform this study, tracks are split at the point of closest approach to the nominal beamline. The top and bottom legs are treated as two independent tracks and re-fitted accordingly. The track parameters are then propagated to their respective points of closest approach to the beamline. This method should be validated using Monte Carlo simulation.

12.4 Hit resolution

The hit resolution is studied by measuring the track residuals, which are defined as the difference between the hit position and the track position. The track is deliberately reconstructed excluding the hit under study in order to avoid bias. The uncertainty relating to the track position is much larger than the inherent hit resolution, so a single track residual is not sensitive to the resolution. However, the track position difference between two nearby modules can be measured with much greater precision. Any uncertainty from translational misalignment between the modules is avoided by fitting a Gaussian to the distribution of the differences between the residuals. For the purposes of this study, only events in which the Track Finder reconstructed a single track are used, and only the barrel modules for which the residual rotational misalignment is less than 10

μm are analyzed. The χ^2 probability of the track is required to exceed x% and the tracks must be reconstructed with at least eight hits. In addition, the track momenta are required to be greater than 1 GeV/c, ensuring that the uncertainty arising from multiple scattering is reduced to less than few μm . Remaining uncertainties from multiple scattering and rotational misalignment between the overlapping modules are included as systematic uncertainties in the measurement. The distribution of the differences between the residuals is fitted, with the width containing contributions from the hit resolutions and the uncertainty from the tracking predictions. The latter is subtracted out in quadrature to leave the resolution on the difference of the hit positions between the two modules. As the two modules are expected to have the same resolution, the resolution of a single sensor is determined by dividing by $\sqrt{2}$.

12.5 Vertex reconstruction

Finding the common intersection points between sets of reconstructed tracks allows identification of the interaction point as well the decay vertices of unstable particles produced in the collision. Identifying and reconstructing different vertices within one event relies on precise track reconstruction and helps to study various physics processes. Commissioning of vertex reconstruction algorithms is part of the checkout with beam.

13 Checkout with beam

The objective of the SVT commissioning with beam is to determine the alignment and operational performance of the tracker detector systems using beam interactions. Operation of the system in the presence of magnetic fields and in conjunction with the trigger and data acquisition system and other ancillary systems are studied as well. Commissioning of the SVT with cosmic rays is limited by the data rate. A much larger data sets are available using beam induced particles. These events are used to make a first relative time alignment of different parts of CLAS12 tracker. First, the coarse time alignment is determined by reading out (triggering) several consecutive clock cycles (events). The event with the highest occupancy determines the correct delay of the trigger signal. After that the fine time adjustment is performed. Only one-strip clusters are considered to avoid bias from capacitive coupling and charge sharing between neighboring channels.

For initial tracker spatial alignment the track finding is based on straight line trajectories since the magnet will not be turned on during these runs. As opposed to the cosmic runs where a dedicated cosmic track finding algorithm is used, the standard CLAS12 tracking algorithms can be deployed to find particles passing through all tracking detectors. In order to select isolated tracks, only the low occupancy runs are used for the alignment and tracks are required to point back to the position of the target and have a requirement on minimum number of hits, track angle relative to local uv plane, and χ^2 per degree of freedom. Outlying hits with large normalized residuals are removed. The initial position of the detector is taken from survey measurements. Then, a pre-alignment is done by connecting hits in the first and last layer of the tracker and calculating the distances to the hits in the other layers. The distributions of these distances will show clear peaks due to real tracks on top of a combinatorial background. This allows to coarse align the layers for the most sensitive axis (x-axis). After this pre-alignment, the track finding algorithm

and the actual alignment are performed. Since the SVT contains only 3 layers, it is hardly possible to do a standalone track reconstruction. Hence, the alignment of the SVT relies on extrapolated tracks from the other tracking detectors (Micromegas and CTOF). The alignment algorithm for the SVT using tracks fitted with a Kalman filter is under development. Each of the SVT modules is aligned for translations along **x** (horizontal) and **y** (vertical) and rotations around the **z** axis. An estimate for the alignment accuracy is obtained from the distribution of the mean of the unbiased track-hit residuals for each detector module, taken from an independent data sample. The next step in alignment procedure is to acquire data with magnet-on and compare the alignment constants with magnet-off data. A cut on minimum momentum is also applied at this stage. Minor differences are expected as some of the detectors might be moving when magnet is turned on. The reconstructed differences should not exceed the expected movements. The spatial alignment on the module level will continue as more statistics is available in order to include more degrees of freedom. The width of alignment residuals is compared with MC predictions.

The performance of the tracker, as well as the trigger and data acquisition system at different beam/target conditions are studied. This includes measurement of rates in all SVT regions at different levels of the solenoid field, and checking for possible saturation effects. Tracker alignment is verified by operating CLAS12 without magnetic fields and at beam currents <0.1 nA to avoid the intense Møller background. Using thin targets will provide a point-like source of charged tracks emerging from the nominal CLAS12 center. SVT is calibrated using beam interactions in a thin target and for various field settings in the CLAS12 Solenoid magnet. This includes validation of trigger and measurement of tracker efficiencies and occupancies. Checkout of the tracker calibration and online reconstruction software is performed. Performance of the tracking and reconstruction software is validated on peaks of known resonances. The mass resolution improves with better alignment.

Bibliography

CLAS note 2010-16, CLAS12 Silicon Vertex Tracker Quality Assurance / Quality Control.

Commissioning the CLAS12 Experimental Equipment, v2, Sep 2011

L.Feld et al., Measurement of common mode noise in binary read-out systems, NIM A 487 (2002) 557-564.

The ATLAS Semiconductor Tracker Collaboration. Beam tests of ATLAS SCT silicon strip detector modules. NIM A 538 (2005) 384-407.

Detector Commissioning Information

System Name

Silicon Vertex Tracker (SVT)

Contact Person

Yuri Gotra <gotra@jlab.org>

System commissioning procedure:

Enter information on the procedure that will be followed to commission the detector, dividing the operation according to three phases:

- (1) quality assurance and system checkout,
- (2) commissioning without beam,
- (3) commissioning with beam.

1. Quality assurance and system checkout procedure:

1.1 Quality assurance

Describe the procedure that will be followed during the construction of the system and its installation in Hall B to ensure the proper functioning of the device, verify alignment and positioning, identify and replace faulty components, For each test that is foreseen provide the following information.

For each individual module:

Test 1: Mechanical survey

Test 2: Module performance test at Fermilab: sensor leakage current, LV current, register test, gain calibration, and noise measurements

Test 3: Module reception test at JLAB: sensor leakage current, LV current, register test, gain calibration, and noise measurements

For a set of modules in a dedicated cosmic ray test stand:

Test 4: Tracking and hit efficiencies, noise occupancies, alignment, and spatial resolution measurements with cosmic rays

For a set of modules in a dedicated test beam setup:

Test 5: Tracking and hit efficiencies, noise occupancies, alignment, and spatial resolution measurements with beam particles

After integration of the barrel on the SVT mechanical structure:

Test 6: Survey of module positions on the barrel and the barrel itself

Test 7: Cosmic run with full barrel in nominal configuration (with full electronics chain)

After integration of SVT with Micromegas (MM), full checkout of the Tracker:

Test 8: Alignment and Survey of SVT versus MM

Test 9: Cosmic run with both tracking systems, cross-talk, noise measurements, alignment, tracking and hit efficiencies, occupancies, resolutions, temperature measurements

After integration of full Central Detector:

Test 10: Cosmic runs with all systems on (magnet on/off)

TEST #1	
Description	<i>Mechanical survey</i>
Special equipment	<i>Optical CMM (at Fermilab)</i>
DAQ Configuration and Trigger	<i>No DAQ</i>
Manpower and time needed	<i>For each module: 30 min (part of module assembling procedure)</i>
Software for analysis of results	<i>MySQL and scripts</i>
Computing resources	<i>None</i>
Information to be saved in the database	<i>Module dimensions, flatness, position of mounting pins, sensor locations</i>

TEST #2	
Description	<i>Module performance test (at Fermilab)</i>
Special equipment	<i>SVT DAQ (VME based), LV and HV PS (MPOD)</i>
DAQ Configuration and Trigger	<i>Local DAQ, configuration files</i>
Manpower and time needed	<i>Per module: 1 man.days Total: 94*1 = 94 man.days</i>
Software for analysis of results	<i>ROOT software</i>
Computing resources	<i>Moderate</i>
Information to be saved in the database	<i>Gain, noise, currents, channel faults</i>

TEST #3	
Description	<i>Module reception test (at JLAB)</i>
Special equipment	<i>SVT DAQ (VME based), LV and HV PS (MPOD)</i>
DAQ Configuration and Trigger	<i>Local DAQ, configuration files</i>
Manpower and time needed	<i>Per module: 2 hours Total: 94*2/8 = 24 man.days</i>
Software for analysis of results	<i>ROOT software</i>
Computing resources	<i>Moderate</i>
Information to be saved in the database	<i>Gain, noise, currents, channel faults</i>

TEST #4	
Description	<i>Efficiencies, alignment, spatial resolution measurements on a dedicated cosmic test stand with cosmic rays</i>
Special equipment	<i>Cosmic test bench (Scintillator paddles + PM)</i>
DAQ Configuration and Trigger	<i>VME based SVT DAQ, Scintillator trigger</i>
Manpower and time needed	<i>Installation + check-out: 5 man.days Data taking: 10 days Data analysis: 10 days Total (man.days): 10 + 5 + 10 = 25 man.days Total (days): ~20 days</i>
Software for analysis of results	<i>ROOT analysis software</i>
Computing resources	<i>Moderate, analysis farm at JLAB</i>
Information to be saved in the database	<i>Gain, noise calibrations, alignment constants, efficiency, spatial resolutions</i>

TEST #5	
Description	<i>Efficiencies, alignment, spatial resolution measurements on a dedicated beam test setup with beam particles using beam telescope in magnetic field</i>
Special equipment	<i>Beam telescope, trigger planes (Scintillator paddles + PM), superconducting magnet</i>
DAQ Configuration and Trigger	<i>VME based SVT DAQ, Scintillator trigger</i>
Manpower and time needed	<p><i>Installation + check-out: 40 man.days</i></p> <p><i>Data taking: 10 days</i></p> <p><i>Data analysis: 60 days</i></p> <p><i>Total (man.days): $40 + 10 + 60 = 110$ man.days</i></p> <p><i>Total (days): ~ 70 days</i></p>
Software for analysis of results	<i>CLARA event reconstruction/tracking software, ROOT analysis software</i>
Computing resources	<i>Moderate, analysis farm at JLab</i>
Information to be saved in the database	<i>Gain, noise calibrations, alignment constants, efficiency, spatial resolutions</i>
TEST #6	
Description	<i>Survey of the SVT barrel (clean room JLab)</i>
Special equipment	<i>Survey equipment</i>
DAQ Configuration and Trigger	<i>None</i>
Manpower and time needed	<i>10 man.days</i>
Software for analysis of results	<i>Survey software</i>
Computing resources	<i>None</i>
Information to be saved in the database	<i>Barrel geometry, module positions</i>

TEST #7	
Description	<i>Cosmic run with full barrel</i>
Special equipment	<i>Cosmic test bench (Scintillator paddles + PM)</i>
DAQ Configuration and Trigger	<i>VME based SVT DAQ, Scintillator trigger</i>
Manpower and time needed	<p><i>Installation + check-out: 5 man.days</i></p> <p><i>Data taking and analysis: 35 days</i></p> <p><i>Total (man.days): $15 * 6 + 5 + 20 * 2 = 135$ man.days</i></p> <p><i>Total (days): ~45 days</i></p>
Software for analysis of results	<i>ROOT analysis software</i>
Computing resources	<i>Medium, analysis farm at JLAB</i>
Information to be saved in the database	<i>Gain, noise calibrations, alignment constants, efficiency, spatial resolutions</i>
TEST #8	
Description	<i>Alignment and Survey of SVT versus MM</i>
Special equipment	<i>Survey equipment</i>
DAQ Configuration and Trigger	<i>None</i>
Manpower and time needed	<i>2 man.days alignment + 2 man.days survey</i>
Software for analysis of results	<i>Survey software</i>
Computing resources	<i>None</i>
Information to be saved in the database	<i>Geometry</i>

TEST #9	
Description	<i>Cosmic rays with both tracking systems</i>
Special equipment	<i>Scintillator paddles, temperature probes</i>
DAQ Configuration and Trigger	<i>MSVT Stand-alone DAQ, Scintillator trigger</i>
Manpower and time needed	<i>Installation + check-out: 20 man.days</i> <i>Data taking: 20 days</i>
Software for analysis of results	<i>ROOT analysis software, CLAS12 Tracking software</i>
Computing resources	<i>Medium, JLAB Computer Farm</i>
Information to be saved in the database	<i>Alignment constants, calibrations, slow controls, run DB</i>

TEST #10	
Description	<i>Cosmic rays with all systems on (Magnet on/off)</i>
Special equipment	<i>Scintillator paddles (to be defined)</i>
DAQ Configuration and Trigger	<i>MSVT Stand-alone DAQ, Scintillator trigger</i>
Manpower and time needed	<i>Data taking: 30 days</i>
Software for analysis of results	<i>ROOT analysis software, CLAS12 Tracking software</i>
Computing resources	<i>Medium, JLAB Computer Farm</i>
Information to be saved in the database	<i>Alignments, calibrations, slow controls, run info</i>

1.2. System Checkout

Describe the checks that will be performed upon completion of installation to verify the proper functioning of the system.

For detector systems, subdivide the information according to the following categories:

- 1) *Checkout of Front-End electronics*
- 2) *Checkout of the High-Voltage system and distribution*
- 3) *Checkout of the Low-Voltage System*
- 4) *Checkout of DAQ and Trigger*

For each, provide the following information.

More checkouts:

- 5) *Checkout of gas system*
- 6) *Checkout of safety system (interlock LV/HV/cooling/gas/magnet quench)*

Checkout of Front-End Electronics	
Description	<i>Calibrations, channel mapping, noise occupancies, trigger rate stress test, stability over time, immunity to condition change, etc.</i>
Manpower and time needed	<i>15 man.days</i>
Software for analysis of results	<i>CLAS12 DAQ, CLAS12 slow control</i>
Computing resources	<i>Computer farm, moderate amount of disk space for data</i>
Dependencies from other systems	<i>Gas, LV and HV system, DCS</i>
Information to be saved in the database	<i>Channel maps, calibration constants, slow control data</i>

Checkout of High-Voltage system and distribution	
Description	<i>Plug the detector to HV supply, check ENC, leakage current monitoring</i>
Manpower and time needed	<i>10 man.days</i>
Software for analysis of results	<i>CLAS12 slow control system</i>
Computing resources	<i>None</i>
Dependencies from other systems	<i>Gas system must be checked-out prior to HV system</i>
Information to be saved in the database	<i>Updated HV distribution map</i>

Checkout of Low-Voltage system for electronics

Description	<i>Low voltage and electronics on, check cable mapping, verification of voltages and currents on all components</i>
Manpower and time needed	<i>5 man.days</i>
Software for analysis of results	<i>CLAS12 slow control system</i>
Computing resources	<i>None</i>
Dependencies from other systems	<i>None</i>
Information to be saved in the database	<i>PS Channel mapping</i>

Checkout of DAQ and trigger

Description	<i>Test of different DAQ and trigger configurations</i>
Manpower and time needed	<i>10 man.days</i>
Software for analysis of results	<i>CLAS12 slow control system, CLAS12 DAQ</i>
Computing resources	<i>Computer farm, moderate amount of disk space for data</i>
Dependencies from other systems	<i>May need other systems for some DAQ configurations (CTOF, MM)</i>
Information to be saved in the database	<i>None</i>

Checkout of gas system

Description	<i>Leak test of gas line (nitrogen), plug detector to gas system, leak test, humidity monitoring</i>
Manpower and time needed	<i>5 man.days</i>
Software for analysis of results	<i>CLAS12 slow control system</i>
Computing resources	<i>None</i>

Dependencies from other systems	<i>DCS, interlocking on dew point</i>
Information to be saved in the database	<i>Leak rates, gas flows and pressures, humidity and temperature data</i>

Checkout of safety system	
Description	<i>Check-out and test interlocks between LV/HV/cooling/gas/magnet quench</i>
Manpower and time needed	<i>15 man.days</i>
Software for analysis of results	<i>CLAS12 DCS system</i>
Computing resources	<i>None</i>
Dependencies from other systems	<i>All systems interlocked</i>
Information to be saved in the database	<i>None</i>

2. Commissioning without beam

2.1. Special calibration procedures

Describe special runs and procedures that will be performed to get first calibration data for the system. These may include pedestal runs, laser runs, measurement with radioactive sources etc. For each, provide the requested information.

Special Run #1	
Description	<i>Calibration run</i>
Goal	<i>Gain, noise</i>
DAQ Configuration and Trigger	<i>Internal trigger, SVT DAQ configuration for calibration run</i>
Manpower and time needed	<i>10 man.days</i>
Software for analysis of results	<i>ROOT analysis software needs to be developed</i>
Computing resources	<i>Moderate</i>
Dependencies from other systems	
Information to be saved in the database	<i>Calibration constants</i>

2.2. Calibration with Cosmic rays

Describe the conditions and goals of data taking with cosmic rays for the system in consideration. Make a separate entry for each different run condition (for example if different triggers are foreseen) and specify the outcomes that will be achieved. When describing possible dependencies from other system, specify which other detector systems should be on during this calibration run and what their configuration should be. Specify whether magnet should be on and what the field intensity should be.

Run #1	
Description and goals	<i>Cosmic run with solenoid magnetic field off</i>
DAQ Configuration and Trigger	<i>DAQ cosmic, external (scintillator paddle) trigger</i>
Dependencies from other systems	<i>Several different runs can be taken with different regions on/off for noise studies</i>
Manpower and time needed	<i>Depends on required statistics, can take days for alignment calibration</i>
Software for analysis of results	<i>Track reconstruction software, to be developed by software team</i>
Computing resources	<i>Computer farm, moderate amount of disk space</i>
Information to be saved in the database	<i>Potential update of efficiency maps</i>
Repetition frequency	<i>Once or Twice per run period, or when beam is off for a long time</i>

Run #2	
Description and goals	<i>Cosmic run with solenoid magnetic field on (50% nominal)</i>
DAQ Configuration and Trigger	<i>DAQ cosmic, external (scintillator paddle) trigger</i>
Dependencies from other systems	<i>Several different runs can be taken with different regions on/off for noise studies</i>
Manpower and time needed	<i>Depends on required statistics, can take days for alignment calibration</i>
Software for analysis of results	<i>Track reconstruction software, to be developed by software team</i>
Computing resources	<i>Computer farm, moderate amount of disk space</i>
Information to be saved in the database	<i>Potential update of efficiency maps</i>
Repetition frequency	<i>Once or Twice per run period, or when beam is off for a long time</i>

Run #3	
Description and goals	<i>Cosmic run with solenoid magnetic field on (100% nominal)</i>
DAQ Configuration and Trigger	<i>DAQ cosmic, external (scintillator paddle) trigger</i>
Dependencies from other systems	<i>Several different runs can be taken with different regions on/off for noise studies</i>
Manpower and time needed	<i>Depends on required statistics, can take days for alignment calibration</i>
Software for analysis of results	<i>Track reconstruction software, to be developed by software team</i>
Computing resources	<i>Computer farm, moderate amount of disk space</i>
Information to be saved in the database	<i>Potential update of efficiency maps</i>
Repetition frequency	<i>Once or Twice per run period, or when beam is off for a long time</i>

3. Commissioning with beam

Describe the run conditions and configurations that are foreseen for this system in the initial phases of operation with beam. List the data runs that you plan on doing, specifying the configuration of your system and of the other detectors, DAQ and trigger configuration and describing the parameters that will be monitored (rates, spectra, ...) and the final outcomes. Include all the runs that should be done to check the system and to perform a complete calibration of the detector.

- 1) Thin target runs at several magnetic field values
- 2) Noise occupancy measurements, gain calibration, alignment

Beam Run #1	
Description and goals	<i>Geometry and tracking tuning. Typically a normal electron run, but potentially with thin target(s) such as CH₂ or carbon in order to have well defined z-vertex.</i>
DAQ Configuration and Trigger	<i>Typical CLAS12 main trigger</i>
Dependencies from other systems	<i>All systems should be on</i>
Manpower and time needed	<i>Long runs (4-8 hours) may be needed to have enough statistics</i>
Software for analysis of results	<i>CLAS12 calibration, alignment, and tracking analysis software to be developed</i>
Computing resources	<i>Computer farm, significant amount of CPU time and disk space (to be defined) for raw data processing</i>
Information to be saved in the database	<i>Updated geometry, updated efficiency maps, alignment constants</i>
Repetition frequency	<i>Useful after large configuration changes</i>

Beam Run #2	
Description and goals	<i>Geometry and tracking tuning with B=0 field. Typically a normal electron run, but potentially with thin target(s) such as CH₂ or carbon in order to have well defined z-vertex.</i>
DAQ Configuration and Trigger	<i>Typical CLAS12 main trigger</i>
Dependencies from other systems	<i>All systems should be on</i>
Manpower and time needed	<i>Long runs (4-8 hours) may be needed to have enough statistics</i>
Software for analysis of results	<i>CLAS12 calibration, alignment, and tracking analysis software to be developed</i>
Computing resources	<i>Computer farm, significant amount of CPU time and disk space (to be defined) for raw data processing</i>
Information to be saved in the database	<i>Updated geometry, updated efficiency maps, alignment constants</i>
Repetition frequency	<i>Useful after large configuration changes</i>